



OH and HO₂ radical chemistry during PROPHET 2008 and CABINEX 2009 – Part 1: Measurements and model comparison

S. M. Griffith^{1,2}, R. F. Hansen^{2,3}, S. Dusanter^{1,4,5}, P. S. Stevens^{1,2,3}, M. Alaghmand⁶, S. B. Bertman⁷, M. A. Carroll^{8,9}, M. Erickson¹⁰, M. Galloway^{11,*}, N. Grossberg¹², J. Hottle¹¹, J. Hou¹³, B. T. Jobson¹⁰, A. Kamrath¹¹, F. N. Keutsch¹¹, B. L. Lefer¹², L. H. Mielke^{6,**}, A. O'Brien^{14,***}, P. B. Shepson^{6,15}, M. Thurlow¹⁴, W. Wallace¹⁰, N. Zhang¹³, and X. L. Zhou¹³

¹School of Public and Environmental Affairs, Indiana University, Bloomington, IN, USA

²Center for Research in Environmental Science, Indiana University, Bloomington, IN, USA

³Department of Chemistry, Indiana University, Bloomington, IN, USA

⁴Université Lille Nord de France, 59000, Lille, France

⁵Mines Douai, CE, F59508, Douai, France

⁶Department of Chemistry, Purdue University, West Lafayette, IN, USA

⁷Department of Chemistry, Western Michigan University, Kalamazoo, MI, USA

⁸Department of Chemistry, University of Michigan, Ann Arbor, MI, USA

⁹Department of Atmospheric, Oceanic, and Space Sciences, University of Michigan, Ann Arbor, MI, USA

¹⁰Department of Civil and Environmental Engineering, Washington State University, Pullman, WA, USA

¹¹Department of Chemistry, University of Wisconsin-Madison, Madison, WI, USA

¹²Department of Earth and Atmospheric Sciences, University of Houston, Houston, TX, USA

¹³School of Public Health, State University of New York at Albany, Albany, NY, USA

¹⁴Department of Chemistry and Chemical Biology, Harvard University, Cambridge, MA, USA

¹⁵Department of Earth and Atmospheric Sciences, Purdue University, West Lafayette, IN, USA

* now at: Department of Chemistry and Biochemistry, University of San Diego, San Diego, CA, USA

** now at: School of Public and Environmental Affairs, Indiana University, Bloomington, IN, USA

*** now at: Civil and Environmental Engineering, Princeton University, Princeton, NJ, USA

Correspondence to: S. M. Griffith (stegriff@indiana.edu)

Received: 6 November 2012 – Published in Atmos. Chem. Phys. Discuss.: 20 December 2012

Revised: 25 April 2013 – Accepted: 3 May 2013 – Published: 3 June 2013

Abstract. Hydroxyl (OH) and hydroperoxyl (HO₂) radicals are key species driving the oxidation of volatile organic compounds that can lead to the production of ozone and secondary organic aerosols. Previous measurements of these radicals in forest environments with high isoprene, low NO_x conditions have shown serious discrepancies with modeled concentrations, bringing into question the current understanding of isoprene oxidation chemistry in these environments.

During the summers of 2008 and 2009, OH and peroxy radical concentrations were measured using a laser-induced fluorescence instrument as part of the PROPHET (Program for Research on Oxidants: PHotochemistry, Emissions,

and Transport) and CABINEX (Community Atmosphere-Biosphere INteractions EXperiment) campaigns at a forested site in northern Michigan. Supporting measurements of photolysis rates, volatile organic compounds, NO_x (NO + NO₂) and other inorganic species were used to constrain a zero-dimensional box model based on the Regional Atmospheric Chemistry Mechanism, modified to include the Mainz Isoprene Mechanism (RACM-MIM). The CABINEX model OH predictions were in good agreement with the measured OH concentrations, with an observed-to-modeled ratio near one (0.70 ± 0.31) for isoprene mixing ratios between 1–2 ppb on average. The measured peroxy radical concentrations, reflecting the sum of HO₂ and isoprene-based peroxy radicals,

were generally lower than predicted by the box model in both years.

1 Introduction

The hydroxyl (OH) and hydroperoxy (HO₂) radicals play important roles in tropospheric photochemistry. OH reacts with volatile organic compounds (VOCs) leading to the formation of both HO₂ and organic peroxy radicals (RO₂), which in the presence of nitric oxide (NO) are converted back to OH. This fast cycling of radicals controls many aspects of atmospheric chemistry such as the formation of ozone, the formation of secondary organic aerosols, and the removal of methane and other greenhouse gases, such as hydrofluorocarbons and hydrochlorofluorocarbons that affect the radiative balance of the atmosphere. Because of the central role of HO_x (OH and HO₂) radicals in atmospheric chemistry, it is important to understand their major production and loss pathways to accurately address current issues of air quality and climate change.

Because of their short lifetime in the atmosphere, modeling the chemistry of HO_x radicals is often done with detailed chemical mechanisms embedded into zero-dimensional box models (Heard and Pilling, 2003; Ren et al., 2008 for example) in addition to chemistry-transport models (Pugh et al., 2010; Stavroukou et al., 2010). While there is generally good agreement between measured and simulated HO_x concentrations in urban and remote areas (George et al., 1999; Konrad et al., 2003; Emmerson et al., 2007; Dusanter et al., 2009b), recent efforts to model HO_x concentrations in forested environments characterized by high mixing ratios of biogenic volatile organic compounds, such as isoprene and low mixing ratios of nitrogen oxides (NO_x = NO + NO₂), have shown serious discrepancies with field observations (Tan et al., 2001; Carslaw et al., 2001; Lelieveld et al., 2008; Whalley et al., 2011; Pugh et al., 2010; Kubistin et al., 2010; Martinez et al., 2010; Lu et al., 2012) (Table 1).

For example, observed-to-modeled ratios of OH during the AEROBIC97 campaign in a remote forested area of Greece were 1.7–6.2 at midday, while the agreement with HO₂ concentrations was highly variable with observed-to-modeled ratios in the range 0.1–1.7 (Carslaw et al., 2001; Heard and Pilling, 2003). During the PROPHET98 campaign in a northern Michigan forest, observed-to-modeled ratios of OH and HO₂ concentrations during the daytime were 2.7 and 0.9, respectively (Tan et al., 2001). From the North American based INTEX-A campaign, Ren et al. (2008) reported daytime boundary layer observed-to-modeled OH ratios of 1.5 at isoprene mixing ratios of 500 pptv that rapidly increased to ratios greater than 6 with increasing isoprene mixing ratios. For the GABRIEL campaign in the boundary layer over the Amazon, Lelieveld et al. (2008) reported observed-to-modeled OH ratios of 5–10, while Kubistin et al. (2010) us-

ing a simpler photochemical box model reported observed-to-modeled OH and HO₂ ratios of approximately 12 and 4, respectively.

In contrast to these isoprene-rich environments, HO_x concentrations measured in forest environments with lower mixing ratios of isoprene were found to be in better agreement with modeled values. For example, Ren et al. (2006) reported measured HO_x concentrations for the PMTACS-NY campaign with observed-to-modeled ratios of 0.82 and 1.21 for OH and HO₂ for daytime isoprene mixing ratios less than 1 ppbv. Kanaya et al. (2007) also reported observed-to-modeled ratios of 1.4 and 1.9 for OH and HO₂ in an environment with low to moderate NO_x levels (Median daytime [NO] = 74 pptv) at isoprene mixing ratios generally less than 500 pptv (Qi et al., 2007). This increase in the observed-to-modeled ratio for OH with increasing isoprene mixing ratios in low NO_x environments may suggest that the radical chemistry in the isoprene oxidation mechanism is incomplete (Ren et al., 2008; Lu et al., 2012). Recent studies have suggested that the observed discrepancy between the measured and modeled concentrations of OH could be reconciled if 40–80 % of the OH radicals were efficiently recycled in the isoprene oxidation mechanism (Lelieveld et al., 2008; Butler et al., 2008).

This study reports measurements and model simulations of HO_x radical chemistry for a forested site in northern Michigan during the 2008 PROPHET (Program on Oxidants: Photochemistry, Emissions, and Transport) and 2009 CAB-INEX (Community Atmosphere Biosphere Interactions Experiment) field campaigns. This work compares the HO_x radical concentrations from these two field campaigns with previous studies, and discusses the ability of a model incorporating the Regional Atmospheric Chemistry Mechanism updated by the Mainz Isoprene Mechanism to reproduce the field observations.

2 Experimental methods

The mixed deciduous forest at the PROPHET site has been described elsewhere (Carroll et al., 2001; Ortega et al., 2007) and consists primarily of high isoprene emitting species such as aspen and oak but also species that emit monoterpenes and sesquiterpenes such as pine and birch. Daytime NO mixing ratios at the site were generally below 70 pptv, with an average morning peak around 150 pptv in 1998 (measured at the same site during PROPHET 1998, Tan et al., 2001), 2008, and 2009, which is likely the result of surface-layer transport and slow upward mixing from soil NO_x emissions (Alaghmand et al., 2011), followed by photolysis of NO₂. These chemical characteristics in combination with a historical record of previous campaigns including radical measurements at the site (Carroll et al., 2001; Tan et al., 2001; Mihele and Hastie, 2003), make the PROPHET site an ideal location

Table 1. Published field campaigns incorporating HO_x measurements in or above forest environments.

CAMPAIGN	PLATFORM	[C5H8] (ppbv)	[NO] (pptv)	OBS/MODEL OH	OBS/MODEL HO ₂ ^a	MODEL MECHANISM	REFERENCES
AEROBIC 1997 ^b	Ground	≤ 2.0	60–100 ^c	1.7–6.4	0.1–1.7	MCM ^d	Carlaw et al. (2001)
PROPHET 1998	Ground	1.0–2.5	30–150	2.66 ^e	0.85 ^e	RACM ^f	Tan et al. (2001)
PMTACS-NY 2002	Ground	< 1.0	40–150 ^g	0.82	1.21	RACM ^h	Ren et al. (2006)
Rishiri Is. 2003 ⁱ	Ground	< 0.5 ^j	10–1000 ^k	0.74 ^l	0.53 ^l	RACM ^m	Kanaya et al. (2007)
INTEX-A 2004	Aircraft	~ 0.1–2.5 ⁿ	< 20 – 2000 ⁿ	0.95 ^o	1.28 ^o	LaRC ^p	Ren et al. (2008)
GABRIEL 2005	Aircraft	2.0 ^q	20 ^q	~ 6–56 ^r	– ^s	MESSy w/MIM	Lelieveld et al. (2008)
Pearl River Delta 2006	Ground	1–6 ^t	140–40 K ^t	1.0–8.0	– ^u	RACM-MIM-GK ^v	Lu et al. (2012)
OP3-Danum 2008	Ground	0.4–1.7 ^w	20–80 ^x	2–3 ^y	~ 1.5 ^{y,z}	CI ² TYCAT(aa) w/MIM2 ^{ab}	Pugh et al. (2010)
BEARPEX 2009	Ground	1.7 ^{ac}	74 ^{ac}	– ^{ad}	– ^{ad}	RACM2 ^{ac}	Mao et al. (2012)

Data reported in this table is for daytime measurements only; ^a HO₂ measurements from these earlier campaigns may be upper limits due to a potential RO₂ interference; ^b Reported for 1100–1500 of 4 measurement days; ^c Heard and Pilling (2003); ^d Jenkin et al. (1997) with updated isoprene and α -pinene degradation schemes (Carlaw et al., 2001; Jenkin et al., 2000); ^e Tan et al. (2001); ^f Stockwell et al. (1997) with more detailed isoprene and terpene chemistry (Tan et al., 2001); ^g Estimated from Ren et al. (2006); ^h Stockwell et al. (1997) and updated with Sander et al. (2003); ⁱ 9 a.m.–5 p.m. values; ^j Qi et al. (2007); ^k Estimated from Kanaya et al. (2007); ^l Kanaya et al. (2007); ^m Stockwell et al. (1997) and updated with monoterpene chemistry from Kanaya et al. (2002); ⁿ Estimated from Ren et al. (2008) and given as the range throughout the planetary boundary layer; ^o Ren et al. (2008) given as the median throughout the planetary boundary layer; ^p Langley Research Center model as described in Crawford et al. (1999); Olson et al. (2004); ^q Given as the daytime mean boundary layer value over the tropical forest (Lelieveld et al., 2008); ^r Estimated from Lelieveld et al. (2008); ^s Lelieveld et al. (2008) gives the measured mean boundary layer HO₂ concentration but not the modeling results; ^t Estimated from Lu et al. (2012); ^u Lu et al. (2012) did not report the Obs/Model HO₂^{*} ratios due to the uncertainty in the interference; ^v Based on Stockwell et al. (1997) and updated with Geiger et al. (2003), and Karl et al. (2006); ^w 75 m height; ^x 5 m height; ^y Compared to base model when unconstrained to observed NO; ^z Comparing HO₂ + RO₂ observed with model; ^{aa} Emissions driven model, not constrained by observed concentrations (Wild et al., 1996; Evans et al., 2000); ^{ab} Taraborelli et al. (2009); ^{ac} 9a–3p campaign average (Mao et al., 2012); ^{ad} Mao et al. (2012) did not report the Obs/model OH and HO₂ ratios, but campaign average comparisons show all daytime model OH points within the 2 σ uncertainty of the measurements when using a chemical modulation technique to measure OH. HO₂ is overpredicted but appears to be within the 2 σ uncertainty of the measurements; ^{ae} Stockwell et al. (2008).

for investigating HO_x radical chemistry in an isoprene-rich, low-NO_x environment.

The PROPHET 2008 campaign was focused on measurements above the forest canopy while the CABINEX 2009 campaign included measurements both above and below the canopy. The work presented here focuses only on the above canopy measurements from 2008 and 2009 which were performed at the top of the 31 meter tower, approximately 8–10 m above the canopy. While both campaigns were well instrumented (Table 2), a more extensive dataset of VOCs and photolysis rate constants were available for CABINEX.

During PROPHET 2008, isoprene, methyl vinyl ketone, methacrolein, and the sum of monoterpenes (C₁₀H₁₆) were measured with a proton-transfer reaction linear ion trap instrument (PTR-LIT) from Purdue University (Mielke et al., 2010). Formaldehyde (HCHO) was measured using a laser-induced fluorescence instrument by the University of Wisconsin (Hottle et al., 2009), and NO_x was measured using a custom-built chemiluminescence analyzer from Purdue University (Alaghmand et al., 2011). The actinic flux in the range of 295–385 nm was measured by an Eppley radiometer (U. of Michigan), and $J(\text{NO}_2)$ values were derived using a correlation of the measured actinic flux and a parameterization (Saunders et al., 2003) for $J(\text{NO}_2)$ on a clear day. Clear sky values for the other 23 photolysis frequencies required to constrain the model were estimated with either the same parameterization or the Tropospheric Ultraviolet-Visible (TUV 4.4) model (Madronich and Weller, 1990), and then scaled to the calculated fit of $J(\text{NO}_2)$ derived from the actinic flux measurements.

During CABINEX2009, a proton-transfer reaction mass spectrometer (PTR-MS) from Washington State Univer-

sity measured isoprene, the sum of methyl vinyl ketone and methacrolein (MVK + MACR), the sum of monoterpenes, formaldehyde, acetaldehyde, methanol, methyl hydroperoxide, acetone, toluene, benzene, and the sum of C₂-alkylbenzenes (Jobson and McCoskey, 2010). Nitrogen oxides were also measured by Washington State University using an instrument based on chemiluminescence of NO and equipped with a blue light photolytic converter for NO₂ measurements (Air Quality Design, Inc.). Carbon monoxide was measured with a Thermo Environmental Instruments Inc. (48C) by the University of Michigan (Carroll et al., 2001). Photolysis frequencies for NO₂, O₃, HONO, H₂O₂, HCHO, and NO₃, were measured by the University of Houston using a Scanning Actinic Flux Spectroradiometer (SAFS) (Flynn et al., 2010) while the remaining photolysis frequencies were estimated as stated above and then scaled to either measured $J(\text{NO}_2)$ or $J(\text{O}^1\text{D})$ values as done previously (Dusanter et al., 2009b).

During both campaigns, glyoxal was measured using a laser induced phosphorescence (LIP) instrument by the University of Wisconsin (Huisman et al., 2008), and ozone was measured using a Thermo Environmental Instruments Inc. (49C) by the University of Michigan. Nitrous acid was measured by the State University of New York-Albany using a wet chemical technique (Huang et al., 2002; Zhou et al., 2011). All of the data are presented in eastern daylight time (local time).

2.1 Measurements of HO_x concentrations

The Indiana University Fluorescence Assay by Gas Expansion (IU-FAGE) instrument has been described in detail

Table 2. Instrumentation used to measure above canopy concentrations.

Species	PROPHET 2008		CABINEX 2009	
	Instrumentation (Institution)	Time resolution (min)/ Uncertainty (%, 1σ) ^a /LOD (ppbv)	Instrumentation (Institution)	Time resolution (min)/ Uncertainty (%, 1σ) ^a /LOD (ppbv)
Hydroxyl radical	IU-FAGE (Indiana U.)	120/20/6E ^{-5b}	IU-FAGE (Indiana U.)	120/20/4E ^{-5c}
Hydroperoxy radical	IU-FAGE (Indiana U.)	0.5/20/6E ^{-4d}	IU-FAGE (Indiana U.)	0.5/20/6E ^{-4e}
Ozone	UV Absorption (U. of Michigan)	1/2/1	UV Absorption (U. of Michigan)	1/2/1
Carbon monoxide	N/A	N/A	(U. of Michigan)	1/6/40
Sulfur Dioxide	N/A	N/A	(U. of Houston)	5/1/0.027
Nitrous Acid	Scrub-AzoDye (SUNY- Albany)	30/7.5/0.001	Scrub-AzoDye (SUNY- Albany)	30/7.5/0.001
Nitric Oxide	(Purdue U.)	10/10/0.017	(Wash. St. U.)	1/8/0.002
Nitrogen Dioxide	(Purdue U.)	10/10/0.017	(Wash. St. U.)	1/12/0.002
Isoprene	PTR-LIT (Purdue U.)	10/15/0.1	PTR-MS (Wash. St. U.)	1/10/0.05
Methacrolein + Methyl Vinyl Ketone	PTR-LIT (Purdue U.)	10/15/0.15	PTR-MS (Wash. St. U.)	1/10/0.07
Total Monoterpenes	PTR-LIT (Purdue U.)	10/15/ 0.11	PTR-MS (Wash. St. U.)	1/10/0.07
Glyoxal	LIP (U. of Wisconsin)	1/20/0.003	LIP (U. of Wisconsin)	1/20/0.004
Formaldehyde	LIF (U. of Wisconsin)	12/40/0.120	PTR-MS (Wash. St. U.)	1/20/0.14
Acetaldehyde	N/A	N/A	PTR-MS (Wash. St. U.)	1/10/0.09
Acetone + 2-Butanone	N/A	N/A	PTR-MS (Wash. St. U.)	1/10/0.12
Toluene, Benzene, ethylbenzenes	N/A	N/A	PTR-MS (Wash. St. U.)	1/10/0.04
Methyl Peroxide	N/A	N/A	PTR-MS (Wash. St. U.)	1/10/0.05
$j(\text{NO}_2)$	Eppley rad. (U. of Michigan)	1/50/-	SAFS (U. of Houston)	1/30/-
$j(\text{O}^1\text{D})$, $j(\text{H}_2\text{O}_2)$, $j(\text{HCHO})$, $j(\text{NO}_3)$	N/A	N/A	SAFS (U. of Houston)	1/30/-

^a OH and HO₂^{*} measurement uncertainty is the calibration uncertainty (1σ). Precision uncertainties on OH and HO₂^{*} measurements are given throughout the text. Other measurement uncertainties in this table may reflect a combined uncertainty from precision and accuracy ^b $1.5 \times 10^6 \text{ cm}^{-3}$; ^c $1.0 \times 10^6 \text{ cm}^{-3}$; ^d $1.5 \times 10^7 \text{ cm}^{-3}$, 30 s measurements are only sampled approximately every 30 min; ^e $1.5 \times 10^7 \text{ cm}^{-3}$, 30 sec measurements are only sampled approximately every 30 min.

elsewhere (Dusanter et al., 2008, 2009a), thus only a brief description will be given here. Additional information, including recent improvements in the instrument, is included in the Supplement. The FAGE technique detects OH by laser-induced fluorescence after expansion of ambient air to low pressure, enhancing the OH fluorescence lifetime and allowing temporal filtering of the OH fluorescence from laser scatter (Heard and Pilling, 2003).

The laser system consists of a Spectra Physics Navigator II YHP40-532Q diode-pumped Nd:YAG laser that produces approximately 5.5 W of radiation at 532 nm at a repetition rate of 5 kHz. This laser pumps a Lambda Physik Scanmate

1 dye laser (Rhodamine 640 in isopropanol) that produces tunable radiation at 616 nm which is frequency doubled to 308 nm. OH radicals are excited using the $Q_1(3)$ transition near 308 nm. During PROPHET 2008, the laser system produced 5–10 mW at 308 nm, while further modifications improved the laser power to 10–15 mW for CABINEX 2009. After exiting the dye laser, the laser beam is focused onto a 50 m fiber optic cable to transmit the radiation to the sampling cell. The net OH fluorescence signal (signal minus background) was determined by successive modulation cycles during which the laser wavelength is successively tuned on-resonance with the OH transition to measure the OH

fluorescence, and off-resonance to measure the background signal. Neuroth et al. (1991) demonstrated that naphthalene had narrow band absorption lines near 308 nm that could interfere with OH measurements and Ren et al. (2004) found that naphthalene had the potential to cause a background interference with the “offline” spectral positions around the $Q_1(2)$ OH transition, resulting in a difference in the magnitude of the background signal on either side of the $Q_1(2)$ transition. However, measurements of the fluorescence spectrum of naphthalene by Martinez et al. (2004) did not reveal a significant transition for naphthalene near the $Q_1(3)$ OH transition. In addition, no elevated signal was observed for either background “offline” position surrounding the $Q_1(3)$ transition during cycling for HO_x measurements in 2008 and 2009, suggesting that spectral interferences were negligible for the measurements reported here. Although most of the OH measurements during PROPHET 2008 and CABINEX 2009 employed the spectral modulation technique described above, an alternative chemical modulation technique was occasionally used to test for unknown interferences and is discussed in Sect. 2.2.

The sampling cell was placed at the top of the 31 m tower, and ambient air was expanded into the detection region through a 1 mm pinhole. The pressure in the cell was maintained at approximately 4.1–7.4 Torr (approximately 5.5–9.9 hPa) using two scroll pumps (Edwards, XDS35i) connected in parallel. A Teflon loop located directly below the inlet allows for the intermittent addition of NO, which converts ambient HO₂ to OH through the fast HO₂ + NO → OH + NO₂ reaction, allowing for indirect detection of HO₂. Interferences from organic peroxy radicals during the HO₂ measurements are discussed in Sect. 2.3. The air stream passes through the central region of the sampling cell where the UV laser beam is reflected back and forth 24 times in a multipass cell (White configuration). The OH fluorescence is collected at right angles to both the air stream and the laser beam and detected using a microchannel plate detector (Hamamatsu R5916U), and a gated detection scheme.

2.2 Performance of the IU-FAGE instrument during the PROPHET 2008 and CABINEX 2009 Campaigns

The 50 m long fiber used to bring the laser light to the sampling cell at the top of the PROPHET tower resulted in a significant loss of laser power (< 10 % transmission) and the generation of after pulses that reduced the sensitivity of the instrument by a factor of approximately 5 compared to previous configurations using a 12 m long fiber. During both campaigns, the laser power entering the IU-FAGE sampling cell was also observed to decrease throughout the campaign, likely due to air temperature fluctuations that led to a shift of the optical fiber mount and a misalignment of the laser beam. In addition, condensation often formed on the entrance window of the multipass cell, degrading the transmission of the optics, likely due to residual impurities left after conden-

sation. A heater was later added to the laser entrance window and fiber mount to attempt to minimize these issues. Measuring the laser power at the exit of the White cell using a photodiode, continuous measurements of the ambient humidity, and performing frequent calibrations allowed the sensitivity of the instrument to be closely monitored, confirming its stability throughout the campaigns. However, the low laser power inside the detection cell (< 1 mW) required the OH measurements during both campaigns to be averaged over 2 h to achieve limits of detection (LOD) of approximately 1.5×10^6 and 1.0×10^6 molecules cm⁻³ ($S/N = 1$) in 2008 and 2009 respectively. Because peroxy radical concentrations are typically 100 times greater than the OH concentrations, the instrument was able to measure their concentrations with a LOD of 2.2×10^7 cm⁻³ and 1.5×10^7 cm⁻³ in 2008 and 2009 ($S/N = 1$, 30 s average). The calibration accuracies (1σ) are $\pm 20\%$ for OH and HO₂ using the water photolysis calibration technique. Additional information regarding the overall uncertainty of the instrument and calibration method can be found in Dusanter et al. (2008, 2009a).

The IU-FAGE instrument was extensively tested in the laboratory to evaluate its sensitivity towards the well-known interference due to laser-photolysis of ozone in the sampling cell (Reaction R1) and the subsequent reaction of O(¹D) with water (Reaction R2):



while this interference is reduced using the FAGE technique (Heard and Pilling, 2003), there is still a measurable interference in the IU-FAGE instrument, likely due to the combination of high laser fluence, beam overlap through the use of the multipass cell, and the large volume of air probed. Based on laboratory calibrations, this interference was equivalent to 8500 (± 800) molecule cm⁻³ of OH when normalized to 1 ppbv of O₃, 1 % of water, and 1 mW of laser power (see Supplement). However, for the above canopy measurements of OH during the PROPHET 2008 and CABINEX 2009 field campaigns, this interference was negligible because of the low laser power (< 1 mW) reaching the sampling cell at the top of the tower through the 50 m fiber, resulting in a predicted laser-generated OH concentration of less than 2.5×10^5 cm⁻³, which was below the detection limit of the instrument at the top of the tower. As a consequence, no correction was applied to the OH measurements presented in this study.

Other potential interferences with OH measurements have been recently investigated during a formal blind intercomparison involving 3 different OH measurement techniques (Schlosser et al., 2009), including LIF-FAGE, Chemical-Ionization Mass Spectrometry (CIMS), and Differential Optical Absorption Spectroscopy (DOAS). Ambient OH measurements made by several LIF-FAGE instruments reported concentrations that were 1.3–1.7 higher than those observed

using the CIMS technique, but generally within the instrument and calibration uncertainties. Chamber measurements of OH by several LIF-FAGE instruments were in good agreement with measurements using the DOAS technique. Except for one instrument consistently measuring 1.7 times higher than the CIMS instrument during the ambient measurements, these results suggest that interferences with the OH measurements in these environments were within the known measurement uncertainty (Schlosser et al., 2009). However, recent measurements of OH using a different LIF-FAGE instrument in a forested environment using an external chemical modulation technique indicated the presence of an unknown interference with measurements of OH, possibly from the oxidation of biogenic VOCs (Huisman et al., 2011; Mao et al., 2012).

A few experiments were performed during CABINEX 2009 to test for interferences with the IU-FAGE instrument located on the forest floor and using a 12 m fiber, resulting in significantly higher laser power in the sampling cell. During separate experiments, both perfluoropropylene (C_3F_6) and carbon monoxide were introduced into a long flow tube that was interfaced to the instrument inlet to scrub ambient OH radicals. This flow tube ensured that there was enough reaction time for ambient OH molecules to be scrubbed before sampling. Any interference was then quantified through measurements of the remaining OH signal when C_3F_6 or CO was added to the flow tube. Only three short tests were carried out around midnight on three different days (1 test each day). The results of these tests suggest the possibility of an interference (in addition to the laser photolysis of ozone and subsequent reaction with water vapor) on the order of $(4-9) \times 10^5 \text{ cm}^{-3}$, potentially accounting for 50–100% of the nighttime OH concentrations measured during these tests. However, it is not clear whether secondary chemistry in the flow tube could lead to the formation of a steady-state concentration of OH, such as from the ozonolysis of alkenes. The IU-FAGE instrument was subsequently tested outdoors in Bloomington, Indiana and at the ground level of the PROPHET site using an automated external C_3F_6 addition using a short ring above the inlet rather than a flow tube to remove ambient OH during the summer of 2010 (see Supplement). In all cases, the measured interference was consistent with that expected from the laser photolysis of ambient mixing ratios of O_3 and subsequent reaction with water vapor (Reactions R1 and R2), suggesting that other potential interferences were negligible. An upper limit of this interference at the highest laser power using the 12 m fiber would have been $5 \times 10^5 \text{ molecules cm}^{-3}$ based on the measured mixing ratios of ozone and water vapor. Additional measurements will be performed in forest environments to determine whether the IU-FAGE instrument is prone to an unknown interference.

2.3 HO₂ interference

Based on previous laboratory investigations and field inter-comparisons, it had been generally believed that the conversion of RO₂ to HO₂ (Reactions R3–R4) in FAGE sampling cells was negligible due to the reduced concentration of oxygen and the short reaction time before detection of OH (Stevens et al., 1994; Mather et al., 1997; Kanaya et al., 2001; Creasey et al., 2002; Heard and Pilling, 2003; Ren et al., 2004; Fuchs et al., 2010):



Previously, Holland et al. (2003) reported a minimal interference ($< 5\%$) coming from methyl peroxy radicals. However, recent studies have reported (Fuchs et al., 2011; Ren et al., 2012) that some hydroxyl alkyl peroxy radicals from the OH-initiated oxidation of alkenes and aromatics can also be detected by chemical conversion through the addition of NO. This is due to the rapid decomposition of the β -hydroxy alkoxy radicals produced from the RO₂ + NO reaction for alkene-based peroxy radicals compared to alkane-based peroxy radicals. These rapid decomposition reactions lead to the formation of a hydroxyalkyl radical, which then reacts quickly with O₂ forming HO₂. As a result, addition of NO to the sampling cell can lead to the conversion of both HO₂ and hydroxyalkyl peroxy radicals to OH (Fuchs et al., 2011).

Calibrations of this interference in the IU-FAGE instrument under the instrumental conditions used during PROPHET 2008 and CABINEX 2009 (inlet size, cell pressure, and NO concentration) indicates that approximately $90 \pm 4\%$ of isoprene-based hydroxyalkyl peroxy radicals are converted to OH in the sampling cell, while less than $20 \pm 2\%$ of propane-based alkyl peroxy radicals are converted (see Supplement). As a result, the IU-FAGE instrument measured the sum of HO₂ and a fraction of organic peroxy radicals ($HO_2^* = HO_2 + \alpha RO_2$, $\alpha \leq 1$) in 2008 and 2009. For the PROPHET environment, isoprene peroxy radicals dominate the hydroxyalkyl peroxy radical population during the daytime (greater than 80% of the model total RO₂ concentration) and thus contribute to the majority of the HO₂ interference in this environment during the day. For the purposes of this paper, measurements of HO₂^{*} will be compared to the sum of hydroperoxy (HO₂) and isoprene-based hydroxy peroxy radicals (ISOP) calculated by the model. However, at night isoprene-based hydroxy peroxy radicals (ISOP) are no longer the dominant peroxy radical. As a result, the measured HO₂^{*} concentration likely reflects the detection of other hydroxyalkyl peroxy radicals in addition to isoprene-based peroxy radicals (see Supplement).

2.4 HO_x modeling using the Regional Atmospheric Chemistry Mechanism (RACM)

HO_x concentrations were simulated using a zero-dimensional box model incorporating the Regional Atmospheric Chemistry Mechanism (RACM) (Stockwell et al., 1997) using the JPL recommended rate constants for the reaction of inorganic species with OH, O₃, and NO₃ (Sander et al., 2011) as described in Dusanter et al. (2009b). In addition, the chemical mechanism was updated with the Mainz Isoprene Mechanism (MIM) (Pöschl et al., 2000; Geiger et al., 2003), which includes a more detailed isoprene oxidation chemistry that is important in low-NO_x environments (Pöschl et al., 2000). Note that this modeling analysis did not incorporate recent additions to the mechanism of isoprene oxidation, such as the formation of epoxides and hydroxyperoxy aldehydes (Paulot et al., 2009; Peeters et al., 2009; Crouse et al., 2011). A detailed analysis of the impacts of these and other proposed additions to the isoprene oxidation mechanism will be examined in a future publication (Griffith et al., 2013).

Table S1 shows the measured and estimated long-lived species for the PROPHET 2008 and CABINEX 2009 campaigns that were used to constrain the model. The modeling of the median campaign data only included those periods when there were simultaneous measurements of both isoprene (ISO) and nitric oxide (NO), as a sensitivity analysis of the model shows that the modeled HO_x concentrations are most sensitive to their concentrations (Table S3 and described below). For PROPHET 2008, the measurements of isoprene and NO were less frequent and often did not overlap, providing just half of the amount of daytime points as in CABINEX 2009 (Table S2). Other important constraints in the model were either measured (as noted above and in Table 2) or estimated depending on their availability in 2008 and 2009 (see Supplement and Table S2).

The differential equations generated from the chemical mechanism were integrated using the FACSIMILE solver with an integration time of 30 h for each data point. This approach insures that all the species affecting HO_x chemistry have reached steady-state. A sensitivity test using a shorter integration time of only 1 h changes the modeled OH, HO₂, and ISOP concentrations by less than 2%. During the integration, the constrained parameters were reinitialized to their initial values every twenty seconds. Sensitivity analyzes were performed on the CABINEX model at the time points 2 a.m., 10 a.m., and 3 p.m. on a number of days from the campaign. To test the sensitivity of the model to constraint concentrations and other key parameter values, the constraints were multiplied by a factor of 2 independently of each other. Table S3 (Supplement) shows the key constraints whose doubling of their concentration leads to more than a 5% change in either OH or HO₂ + ISOP concentrations in the model. The largest effect on OH and HO₂* radical concentrations during the sensitivity analysis comes from ozone, nitric oxide, and

isoprene during the day while at night the largest impact is from doubling ozone mixing ratios with a more limited impact from some alkene mixing ratios. Large impacts during the day can also be seen from temperature, photolysis frequencies, and water mixing ratios.

Uncertainties associated with the modeled HO_x concentrations were calculated from Monte Carlo simulations using rate constants and measured constraint concentrations that were randomly selected from their uncertainty distributions (Carslaw et al., 1999, 2001). All of the individual model points at 10 a.m. ([NO] > 50 pptv) and 3 p.m. ([NO] < 50 pptv) were simulated 600 times each with constraint and rate constant values from the uncertainty distribution, resulting in an uncertainty (relative standard deviation) on average of 42% for OH and 31% for HO₂ + ISOP for the 2008 day-to-day modeling (2σ), but only 32% and 20% for OH and HO₂ + ISOP for the CABINEX 2009 day-to-day modeling. The more comprehensive dataset from CABINEX led to a smaller overall uncertainty on the modeling constraints than in 2008. Simulations done at the 2 a.m. model points during CABINEX reveal a greater uncertainty of 56% and 46% for OH and HO₂ + ISOP at night. The greater uncertainty at night is due to ozone + alkene reactions dominating new radical formation and the absence of comprehensive measurements of non-biogenic alkene mixing ratios, whose mixing ratios are set equal to the median mixing ratios from Tan et al. (2001). Carslaw et al. (2001) used a similar chemical mechanism to calculate OH and HO₂ concentrations in a forest environment and found through the same type of analysis that their day-to-day modeled OH and HO₂ concentrations had an uncertainty of 33% and 20% (2σ), similar to the results from the CABINEX modeling.

3 Results

Figures 1 and 2 display the measured values and model results together with key meteorological and chemical measurements from PROPHET 2008 and CABINEX 2009. The meteorological conditions during the PROPHET 2008 campaign were similar to those observed during previous years (Carroll et al., 2001, 2008), while the CABINEX 2009 campaign conditions could be considered atypical. Temperatures during July 2009 were unseasonably cold, resulting in temperatures approximately 1–2 degrees Celsius lower than in 2008 and 3–4 degrees Celsius cooler than the historical average (Bryan et al., 2012), while the average photolysis rate constants were similar (Fig. 3). The low temperatures observed during CABINEX 2009 may be a factor in the difference between the observed isoprene mixing ratios for the two campaigns (Fig. 3), as temperature has been shown to have both instantaneous and cumulative effects as a driving factor along with UV/visible light in biogenic VOC (BVOC) emissions (Monson et al., 1994; Petron et al., 2001; Sharkey et al., 2001; Blanch et al., 2011), although unknown errors

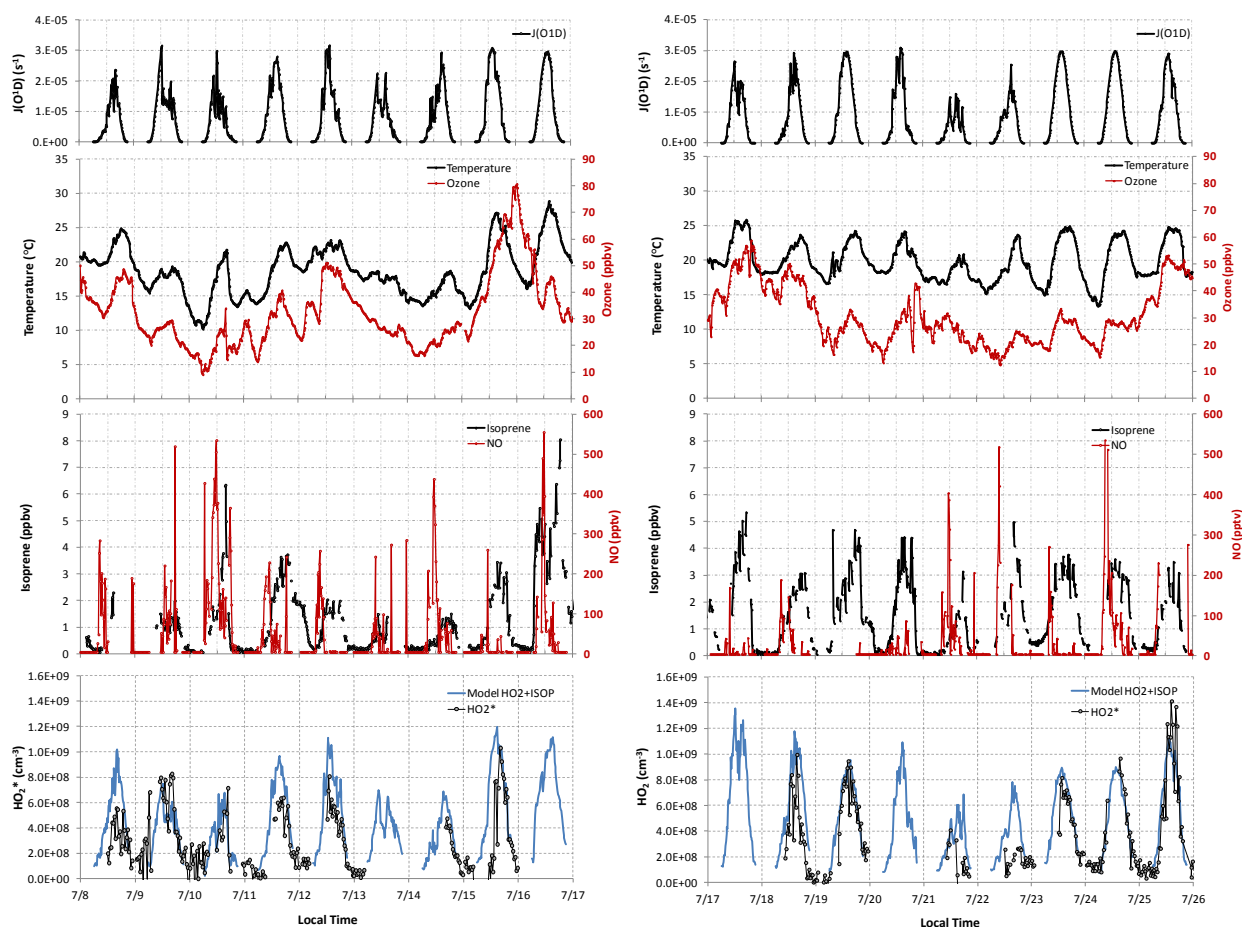


Fig. 1. PROPHET 2008 data showing key model constraints and modeled and measured HO_2^* concentrations. Measured HO_2^* precision (not shown) is approximately $1.5 \times 10^7 \text{ cm}^{-3}$.

associated with the different instrumental techniques cannot be ruled out. The sum of the mixing ratios of methacrolein and methyl vinyl ketone as well as the formaldehyde mixing ratios were greater during PROPHET 2008 (Fig. 3), which may be due to higher precursor isoprene mixing ratios due to higher emissions (Millet et al., 2008). Although the different techniques used to measure isoprene and VOCs during the two campaigns were not compared, each technique has been previously compared to established GC methods (de Gouw and Warneke, 2007; Mielke et al., 2010). Measurements of ozone and NO mixing ratios were similar during both campaigns, while the measured mixing ratio of NO_2 was greater during PROPHET 2008 compared to CABINEX 2009, even though the photolysis rates were similar. Two different instruments were used during the campaigns and the reasons for this discrepancy are unclear. However, any uncertainty associated with the measurements of NO_2 has a minimal impact on the modeled concentrations of OH as the $\text{OH} + \text{NO}_2$ reaction is not a significant sink of OH in this environment (see Sect. 4.3).

3.1 OH and HO_2^* measurements during PROPHET 2008

Because of the low laser power at the top of the tower, the day-to-day measured OH concentrations suffered from poor precision during PROPHET 2008 even after averaging over 2 h and unfortunately do not allow for a meaningful comparison with the model. However, because of the higher concentration of peroxy radicals, the day-to-day measured HO_2^* concentrations for PROPHET 2008 have sufficient precision to compare with the model, and the measured and modeled concentrations are shown in Fig. 1. The measured HO_2^* concentrations for PROPHET 2008 generally agree with the modeled $\text{HO}_2 + \text{ISOP}$ concentration to within the 2σ model uncertainty (Fig. 4a) for 70 % of the points and reasonably reproduces the day-to-day variations (Fig. 1), although the model tends to overestimate the measured concentrations. A linear regression of the points (Fig. 4a) has a slope of 0.69 ± 0.05 and an R^2 value of only 0.31, reflecting the substantial scatter in the data points.

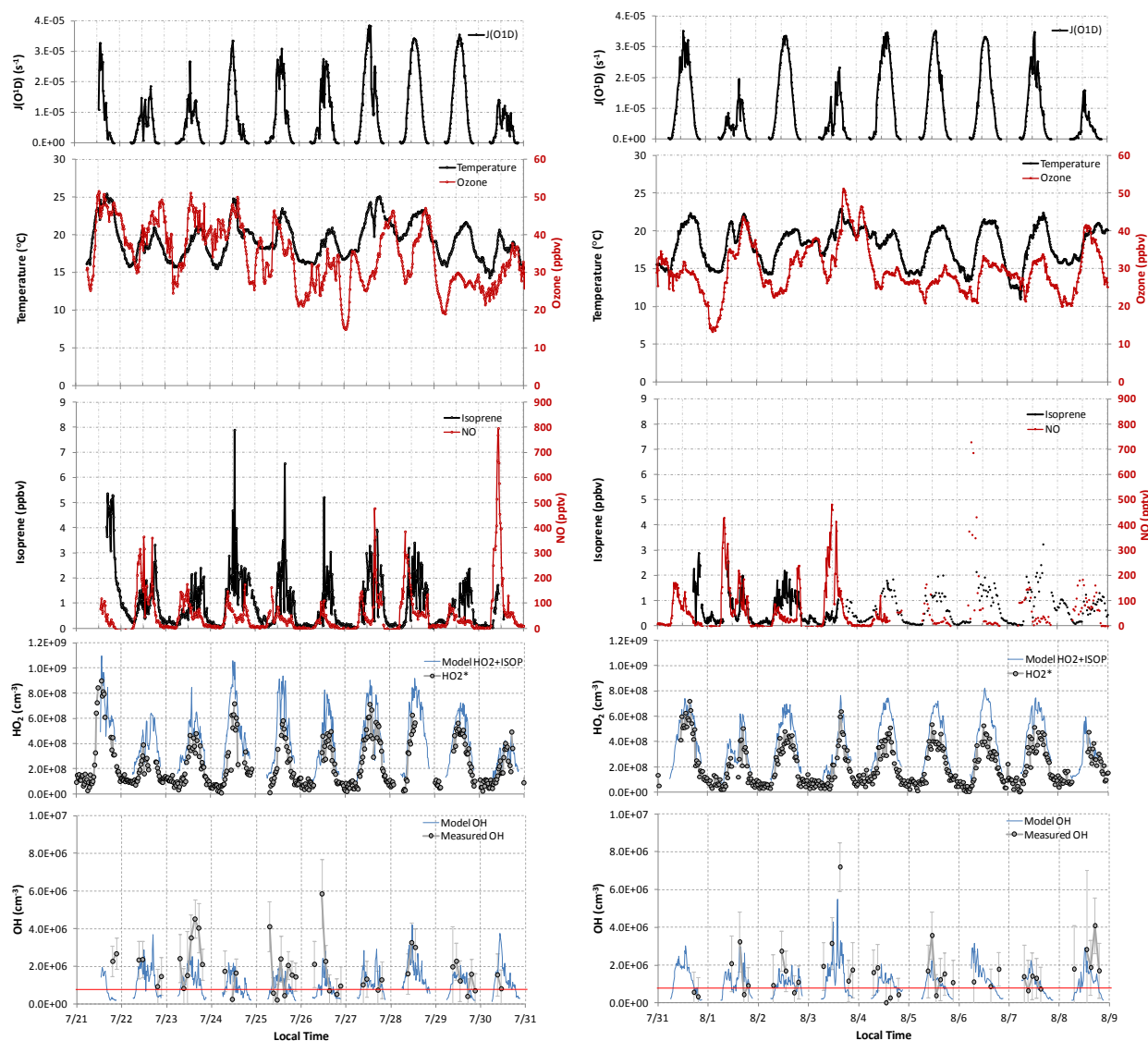


Fig. 2. CABINEX 2009 data showing key constraints and modeled and measured OH and HO₂* concentrations. Error bars on the OH measurements are the 1 σ precision values of each measurement. Measured HO₂* precision (not shown) is approximately 1.5×10^7 cm⁻³. The red line in the OH plot indicates the LOD on the 2 h median measurements (1.0×10^6 cm⁻³). Only positive daytime OH measurements are shown for simplicity.

A 2 h diurnal median of all the OH measurements made during PROPHET 2008 does allow a more meaningful comparison to the model, as shown in Fig. 5 along with the measured and modeled median campaign concentrations of HO₂*. As seen in this figure, the model tends to underpredict the 2 h measured median OH in the afternoon, but the data is highly variable and the precision on each point is still relatively poor (LOD of 1×10^6 cm⁻³ on average), with the model only significantly underpredicting the median measured OH value at mid-afternoon. In contrast, the PROPHET 2008 modeled HO₂ + ISOP tends to overpredict the measured campaign

median HO₂* concentrations, although the difference is generally within the estimated uncertainty of the model (Fig. 5).

3.2 OH and HO₂* measurements during CABINEX 2009

The day-to-day modeled OH and HO₂* concentrations for CABINEX 2009 are shown in Fig. 2. The higher laser power used during CABINEX 2009 (LOD of 1.0×10^6 cm⁻³ on average) resulted in better precision of the daily 2 h average measured OH concentrations compared to the day-to-day measurements of OH during PROPHET 2008 (LOD of 1.5×10^6 cm⁻³ on average), although only between 30–50 %

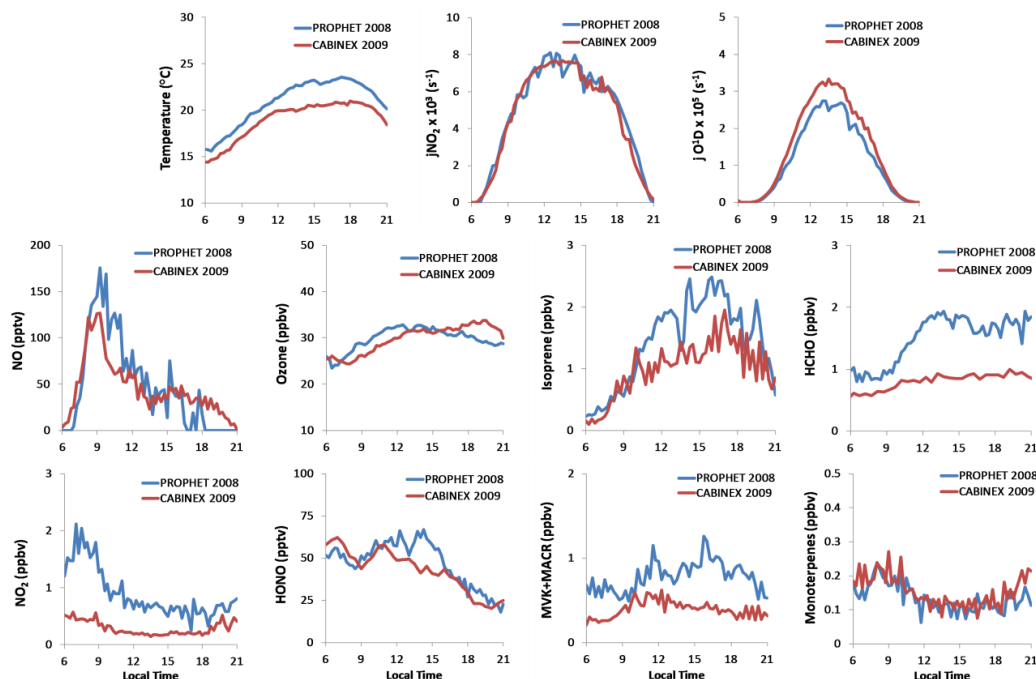


Fig. 3. Diel median values of several species measured from above canopy during PROPHET 2008 (blue) and CABINEX 2009 (red). Constrained model inputs based on overlap of measurements are shown in the Supplement.

of the daytime measurements were different from zero beyond their 2σ uncertainty. Figure 6 displays a correlation plot of the measured vs. modeled OH concentrations for the CABINEX 2009 campaign with a bivariate least-squares regression weighted by the measurement precision and model uncertainty (Cantrell et al., 2008). Even though the correlation is poor, only 11 % of the points are outside the 2σ uncertainty range of the measurements and do not display any systematic trend. The modeled HO_2^* ($\text{HO}_2 + \text{ISOP}$) concentrations are higher than the measurements on several days (Fig. 2), and the measured vs. model correlation plot shown in Fig. 4b illustrates that the model generally overpredicts the measured concentrations, with approximately 50 % of the daytime HO_2^* measurements outside of the 2σ uncertainty of the measurements and the model. The measured nighttime HO_2^* concentrations are well reproduced by the modeled $\text{HO}_2 + \text{ISOP}$ during several nights, while overpredicting the measured concentration on a few nights. A linear regression of the combined daytime and nighttime 2009 data results in a slope of 0.64 ± 0.01 and an R^2 value of 0.86.

The CABINEX 2009 modeled OH concentrations are in good agreement with the 2 h median campaign measured concentrations of OH (precision of $5.5 \times 10^5 \text{ cm}^{-3}$ on average) (Fig. 7). However, similar to the PROPHET 2008 results, the CABINEX 2009 modeled concentrations of $\text{HO}_2 + \text{ISOP}$ are higher than the campaign median measurements of HO_2^* by a factor of 1.3–2.5 throughout the day (Fig. 7), with the daytime measured HO_2^* values just outside of the

lower bound of the model uncertainty (2σ), similar to the 2 h day-to-day HO_2^* comparison (Fig. 4b).

Total OH reactivity was also measured during CABINEX 2009 (Hansen et al., 2013) and can be compared with the total OH reactivity predicted by the model to test the accuracy of the model's OH loss mechanisms. Figure 8 shows the comparison between the median measured and modeled OH reactivity between 26 July and 8 August. As seen in this figure, the model tends to underpredict the measured total OH reactivity by a factor of 1.5–2.0 in the afternoon and generally overpredicts it at night, although at night the model is generally within the 2σ uncertainty of the measurements and the model.

4 Discussion

4.1 OH measurement – model comparison

As summarized in Table 1, previous measurements of OH radical concentrations in forest environments with low mixing ratios of NO_x and high mixing ratios of isoprene are generally significantly greater than model predictions (Tan et al., 2001; Carslaw et al., 2001; Lelieveld et al., 2008; Pugh et al., 2010; Stavrakou et al., 2010; Lu et al., 2012). In contrast to these previous studies, the campaign median measurements of OH from CABINEX 2009 are in good agreement with the model predictions where median peak isoprene mixing ratios were between 1–2 ppbv (Figs. 6 and 7).

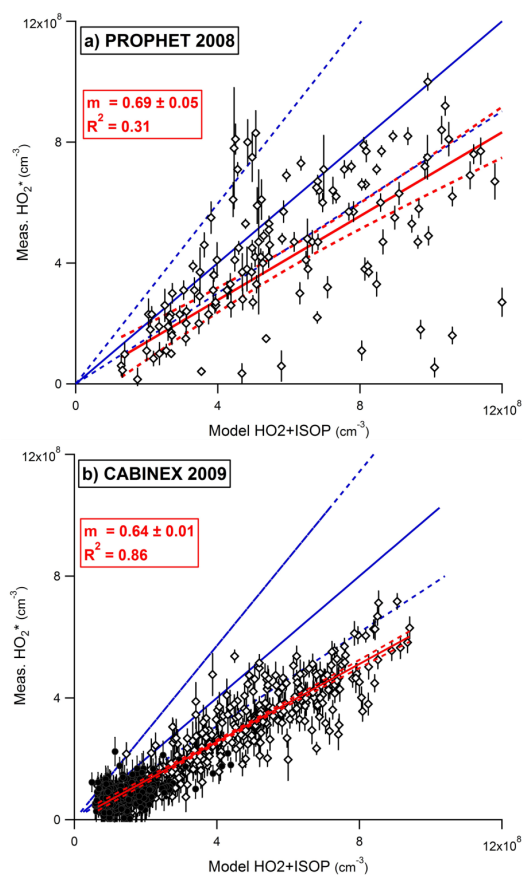


Fig. 4. HO₂* correlation plots for PROPHET 2008 (top) and CABINEX 2009 (bottom, open diamonds = daytime, filled circles = nighttime) showing 30 s measurement values (sampled every 30 min) from each year. The blue lines are the 1 : 1 correlation (solid) and the model HO₂ + ISOP uncertainty (2σ) is shown by the dashed blue lines. The solid red line is a linear regression of the data with 95 % confidence limits shown as dashed red lines. Measurement precision for both years is approximately 1.5×10^7 cm⁻³.

Many of these previous studies found that the discrepancy between the measured and modeled concentration of OH increased with increasing mixing ratios of isoprene (Ren et al., 2008; Kubistin et al., 2010). Although the models used in these studies may have differences in their chemical mechanism (Tan et al., 2001; Kanaya et al., 2007; Lu et al., 2012), or differences in the model implementation (Lelieveld et al., 2008; Pugh et al., 2010) and have not been compared to the present model, an analysis of the CABINEX observed to model OH ratio (Fig. S7) does not reveal a significant dependence on the isoprene mixing ratio, although the precision of the correlation is poor due to the poor precision of the OH measurements. However, recent measurements by Mao et al. (2012) during BEARPEX 09 using a chemical modulation technique to detect OH radicals were significantly lower than measurements using the spectral modulation technique and were in good agreement with model predictions with iso-

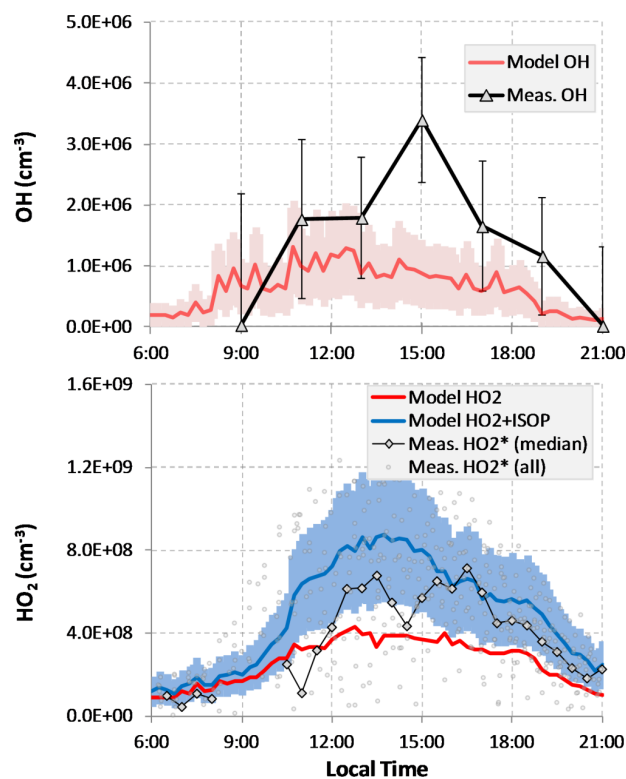


Fig. 5. PROPHET 2008 OH and HO₂* median measurements with the RACM/MIM model results. Measured points are shown as 2 h medians (OH, triangles) and 30 min medians (HO₂*, diamonds) for the daytime measurements (6 a.m.–9 p.m.). Error bars are the 2σ measurement precision for OH, while the HO₂* measurement precision (not shown) is approximately $\pm 2.0 \times 10^7$ cm⁻³. Gray circles in the bottom plot represent all of the HO₂* measurements during PROPHET 2008 while the gray diamonds are the 30 min median for the times of this analysis where HO₂* measurements are available. The red lines represent the base RACM/MIM daytime model results for OH (2σ relative uncertainty ± 50 % shaded) or HO₂. The blue lines represent the daytime modeled HO₂ + ISOP (2σ relative uncertainty ± 33 % shaded).

prene mixing ratios between 1–2 ppb on average, suggesting that there may be an unknown interference associated with the LIF-FAGE technique related to the oxidation of biogenic VOCs. A similar interference could explain the high measurements of OH observed in the afternoon during the warmer PROPHET 2008 campaign coinciding with the maximum afternoon temperature and highest isoprene concentrations. However, any interference in the measurements during CABINEX 2009 presented here would result in a reduction in the measured OH concentrations, leading to an overprediction by the model. This result would still stand in contrast to the general underprediction of measured OH concentrations in forest environments by current atmospheric chemistry models (Table 1).

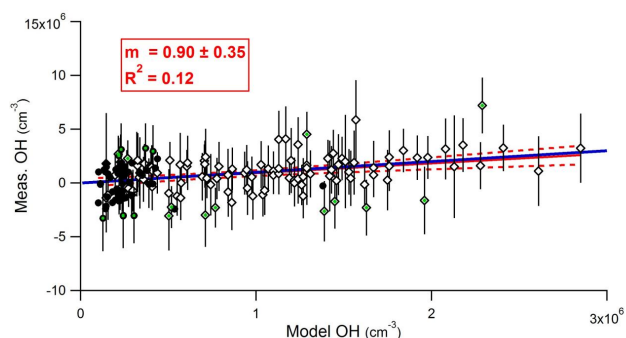


Fig. 6. OH correlation plot for CABINEX 2009 (filled circles = nighttime, open diamonds = daytime) showing 2 h median values. Vertical error bars are 2σ precision values on the measurements. The CABINEX 2σ model uncertainty (40 %) is excluded. Green points are significantly (2σ) outside of the error bar range. Nighttime points within the 2σ uncertainty do not have their precision values shown. The blue line is a 1 : 1 correlation line and the solid red line shows a measurement vs. model regression of the data weighted by the precision in the measurements and the uncertainty of the model concentrations (slope = 0.90 ± 0.35), with dashed red lines representing the 95 % confidence limits of the slope.

The campaign median measured concentrations of OH at night during 2009 were less than $5 \times 10^5 \text{ cm}^{-3}$ ($2.7 \times 10^5 \text{ cm}^{-3}$ on average between 10 p.m. and 6 a.m.), near or below the detection limit of the instrument and approximately four times lower than previously observed at this site (Faloona et al., 2001). The 2 h median night-to-night OH concentrations measured in 2009 are in reasonable agreement with the modeled results (median observed to model ratio = 0.8), although there is significant scatter in the data as the nighttime measurements were generally near the detection limit of the instrument. One possible explanation for the high nighttime concentrations of OH measured previously at this site may be the presence of an unknown interference related to the oxidation of biogenic VOCs. As previously mentioned, recent measurements by the Penn State ground-based HO_x LIF instrument in a ponderosa pine forest found that OH measurements using an external scrubbing technique similar to that described above were 40–50 % lower than measurements using the traditional spectroscopic method, and that the discrepancy was temperature dependent (Mao et al., 2012). As discussed above (Sect. 2.2), it is not clear whether the instrument was sensitive to a similar interference, although the measurements described above at this site using the external scrubbing technique did not reveal a significant interference. However nighttime ozone levels were generally 4–8 ppbv higher on average over the 7 week PROPHET 1998 campaign compared to the 3 weeks of above canopy measurements during CABINEX 2009. In addition, the average temperature was 3–5 °C warmer on average in 1998 compared to 2009. These differences could impact both nighttime radical production as well as potential instrument inter-

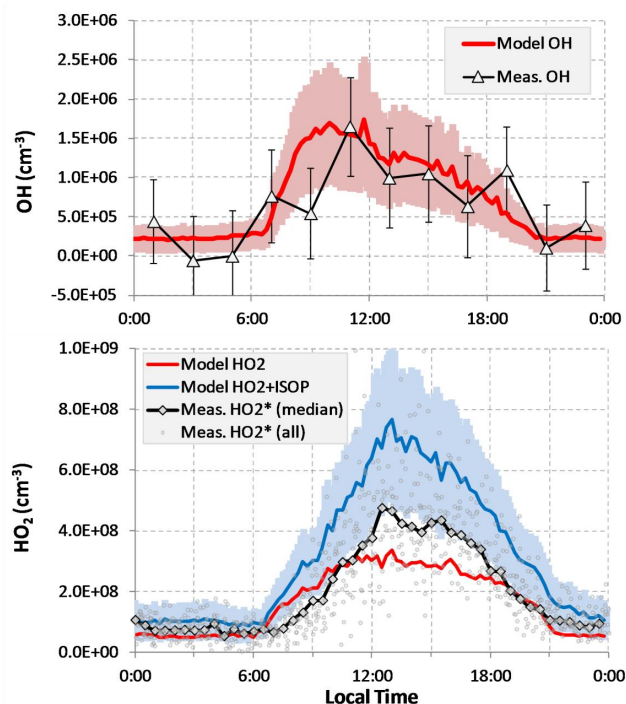


Fig. 7. CABINEX 2009 OH and HO_2^* median measurements with the RACM/MIM model results. Measured points are shown as 2 h medians (OH, triangles) and 30 min medians (HO_2^* , diamonds). Error bars are the 2σ measurement precision for OH, while the HO_2^* measurement precision (not shown) is $\pm 1.5 \times 10^7 \text{ cm}^{-3}$. Gray points in the bottom plot represent the entire above canopy HO_2^* measurements during CABINEX 2009. The red lines represent the base RACM/MIM model results for OH (2σ relative uncertainty $\pm 32\%$ shaded) or HO_2 . The blue lines represent the modeled $\text{HO}_2 + \text{ISOP}$ (2σ relative uncertainty $\pm 30\%$ and $\pm 41\%$ shaded for day and night).

ferences. Unfortunately, laser problems prevented extended measurements of OH at night during 2008, when the observed average nighttime temperatures and ozone levels were between those measured in 1998 and 2009. Other potential instrumental interferences for IU-FAGE associated with VOC oxidation products are being investigated.

The model underprediction of the measured OH reactivity in the afternoon suggests that the model may be missing an additional daytime OH sink. Depending on the nature of the missing reactivity, the modeled OH concentrations may be lower if the model was constrained to the measured OH reactivity. However, increasing the modeled reactivity by systematically increasing the constrained VOC mixing ratios to fit the afternoon measured reactivity only decreases the modeled OH concentrations by 30 % on average, still in good agreement with the measurements during CABINEX 2009 (see discussion below and in the Supplement).

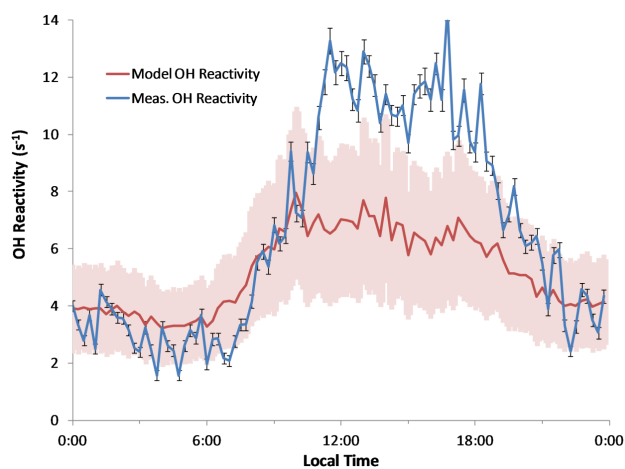


Fig. 8. Measured and modeled median total OH reactivity for the period analyzed for CABINEX 2009 (26 July–8 August). Error bars on the measured points are the 2σ uncertainty values ($\pm 3\% + 0.14 \text{ s}^{-1}$, 50 point median). Pink outline is the 2σ uncertainty ($\pm 40\%$) of the modeled OH reactivity.

4.2 HO₂^{*} measurement – model comparison

Previous measurements of HO₂ concentrations in forested environments were found to be in good agreement with model predictions in some studies (Tan et al., 2001), while significantly underpredicted in others (Lelieveld et al., 2008; Pugh et al., 2008; Stavroukou et al., 2010). However, it is not clear whether these previous HO₂ measurements are free from measurement interferences from β -hydroxyperoxy radicals as discussed above (Fuchs et al., 2011). As discussed above (Sect. 2.3), laboratory calibrations have shown that approximately 90 % of isoprene-based peroxy radicals are detected by the IU-FAGE instrument in addition to HO₂ under the instrumental configurations during PROPHET 2008 and CABINEX 2009. Because the model predicts that isoprene-based peroxy radicals comprise approximately 80 % of the total RO₂ radical pool in this environment, isoprene-based peroxy radicals are the dominant species contributing to the HO₂ interference in these measurements. Figure 9 illustrates the dependence of the observed HO₂^{*} to modeled HO₂ ratio on mixing ratios of NO and isoprene for the measurements during CABINEX 2009. However, when the ratio of the observed HO₂^{*} to the modeled sum of HO₂ + ISOP is plotted versus NO and isoprene, the dependences appear to be significantly reduced (Fig. 9). This is consistent with the IU-FAGE measurements of HO₂^{*} reflecting the concentration of both HO₂ and isoprene peroxy radicals. In addition, the modeled HO₂ + ISOP concentrations better reflects the shape of the median diurnal trends in the measured HO₂^{*} concentrations compared to the modeled HO₂ concentrations (Figs. 5 and 7). The measured HO₂^{*} concentrations during 2008 and 2009 were generally between $2\text{--}14 \times 10^8 \text{ cm}^{-3}$ (Figs. 1 and 2),

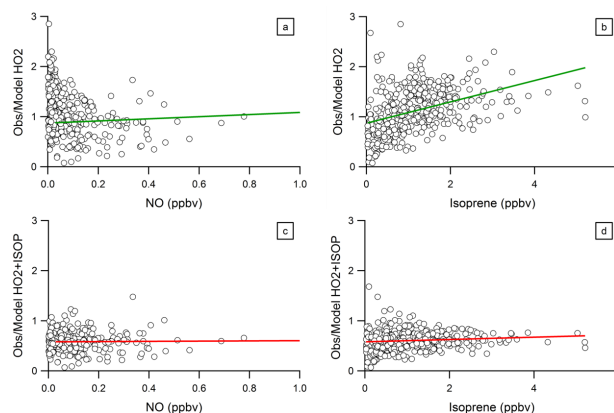


Fig. 9. Daytime (6 a.m.–9 p.m.) measured HO₂^{*}/ modeled HO₂ (top) and measured HO₂^{*}/modeled HO₂ + ISOP (bottom), plotted versus NO (left) and isoprene (right) during CABINEX 2009. Unweighted linear correlations are shown in red and green.

similar to previous measurements of total RO_x (HO_x + RO₂) concentrations at this site in 1997 (Mihele and Hastie, 2003), further suggesting that the measured HO₂^{*} concentrations reflect the sum of HO₂ and isoprene peroxy radical concentrations. The modeled RO₂/HO₂ ratios were between 1.5–2.5 on average, similar to that calculated previously for PROPHET 1998 (Tan et al., 2001).

As illustrated in Figs. 4, 5 and 7, the modeled sum of HO₂ + ISOP tends to overestimate the measured HO₂^{*} concentrations during both 2008 and 2009, although the agreement is better during the warmer PROPHET 2008 campaign than the cooler CABINEX 2009 campaign. The lifetime of HO_x radical reservoir species such as HO₂NO₂ and PAN is greater under the cooler conditions in 2009, and it is possible that the greater observed model-measurement discrepancy of HO₂^{*} during CABINEX is due to the transport of these important radical reservoirs out of the modeling environment, as such loss mechanisms are not accounted for in the zero-dimensional box model. However, adding an additional first-order loss rate of 0.01 s^{-1} for both HO₂NO₂ and PAN to the model (decreasing the lifetime of PAN from approximately 1 h to less than 2 min and the HO₂NO₂ lifetime from approximately 20 s to 16 s) does not have a large impact on the modeled concentrations of HO₂^{*} during CABINEX 2009.

The systematic model overprediction of the observed HO₂^{*} concentrations suggests the possibility of a missing peroxy radical loss mechanism or an overestimation of the peroxy radical production. A recently proposed radical recycling mechanism (Peeters et al., 2009; Peeters and Muller, 2010; Crouse et al., 2011) can lead to a decrease in the concentration of isoprene peroxy radicals through isomerization reactions. Although the radical isomerization decreases the modeled ISOP concentration, the products can lead to a net production of both OH and HO₂ leading to a net increase in the modeled HO₂ + ISOP radical concentrations and thus may

not explain the discrepancy between the measured and modeled HO_2^* concentrations observed here. A detailed discussion of the impact of this and other radical recycling mechanisms (Lelieveld et al., 2008; Hofzumahaus et al., 2009) and a comprehensive analysis of radical production routes and potential missing loss processes for HO_2^* are beyond the scope of this study and will be examined in a subsequent paper (Griffith et al., 2013).

Nighttime HO_2^* concentrations (11 p.m. to 5 a.m.) are in reasonable agreement with the modeled $\text{HO}_2 + \text{ISOP}$ concentration, although the model tends to overpredict the observed campaign median by approximately 35%. However, as discussed above, isoprene peroxy radicals may not be the dominant hydroxyalkyl peroxy radical at night. As a result, this agreement may be fortuitous as it is likely that other peroxy radicals contribute to the measured nighttime concentration of HO_2^* (see Supplement). In addition, the treatment of RO_2 chemistry in RACM is limited and can lead to the accumulation of the concentration of several peroxy radicals under the modeled conditions of this study (Fig. S5). This is in part because of the lack of a complete set of $\text{RO}_x + \text{RO}_x$ radical reactions which would help regulate the nighttime RO_2 concentrations, but are not important during the day when higher mixing ratios of NO and HO_2 control the RO_2 concentrations.

As noted above, the measured OH reactivity is underpredicted by a factor of 1.5–2.0 in the model from 11 a.m. to 5 p.m. It has been previously proposed that the observed missing OH reactivity may be due to the presence of unmeasured reactive biogenic VOCs (DiCarlo et al., 2004). However, these reactions would likely lead to the production of hydroxyalkyl peroxy radicals which would likely contribute to the concentration of HO_2^* and potentially increasing the model measurement disagreement. Constraining the model to the higher measured OH reactivity could improve the observed-to-modeled HO_2^* discrepancy if the increased reactivity routes do not produce detectable peroxy radicals (for example $\text{OH} + \text{saturated alkanes}$ generate RO_2 that are not efficiently detected during the HO_2 measurement); although more than 100 ppb of additional small saturated alkane would be required to close the reactivity budget. Introducing an additional OH loss route as a first order reaction from 11 a.m. to 5 p.m. that does not regenerate another RO_x radical decreases the modeled OH and $\text{HO}_2 + \text{ISOP}$ concentrations by 30–60% and 15–35%, respectively, while adding an OH loss route that proceeds to an alkane RO_2 radical (such as ethane peroxy radical, ETHP), decreases the modeled OH and $\text{HO}_2 + \text{ISOP}$ by 20–50% and 10–25%. The lower modeled OH concentration from the additional OH loss routes during the midday is still within the uncertainty associated with the measured OH; however, the reduction in the modeled $\text{HO}_2 + \text{ISOP}$ concentration is small compared to the 50–70% reduction needed to bring the model into agreement with the measurements at midday, suggesting that the model

is underestimating the loss of $\text{HO}_2 + \text{ISOP}$ or overpredicting a peroxy radical source.

4.3 Radical budgets

A rate of production analysis provides information about the key processes driving radical production and loss routes, which can be divided into initiation, termination and propagation categories to more specifically describe the sources and sinks of OH, HO_2 , RO_2 , HO_x , and RO_x ($\text{HO}_x + \text{RO}_2$, the total sum of radicals). In this study, RO_x radical initiation routes are defined as those leading to new RO_x radical formation, with primary contributions from photolysis routes and ozonolysis of alkenes. RO_x radical termination routes are those that remove RO_x radicals from the system with either RO_x radical + radical or RO_x radical + NO_x reactions dominating termination depending on the mixing ratio of NO_x . Finally, propagation routes convert one RO_x radical into another (e.g., $\text{HO}_2 + \text{NO} \rightarrow \text{OH} + \text{NO}_2$).

Figure 10 illustrates the campaign daytime modeled radical budget for 2008 and 2009 with arrows and rates indicating the direction and magnitude of the RO_x radical initiation, termination, and propagation routes. Given that the model reasonably reproduces the measured OH concentrations, these model derived radical budgets can provide insights into the importance of individual radical sources and sink in this environment, even though, the modeled $\text{HO}_2 + \text{ISOP}$ overpredicts the measured HO_2^* in both years. The rates are 12 h medians from 7.30 a.m.–7.30 p.m. In this figure, arrows pointing towards a radical are considered a component of production (initiation and propagation) and those pointing away are a component of loss (termination and propagation). Figure 10 indicates that the primary radical initiation route at the PROPHET site is the formation of new OH radicals, while the primary radical termination route is through peroxy radical (RO_2 and HO_2) reactions. However, RO_x radical propagation routes are still important compared to initiation and termination routes even in this moderately low NO_x environment, although the average chain length for OH radical propagation is less than one.

Figures 11 and 12 compare the diurnal trends of the median campaign model OH and total radical budgets for PROPHET 2008 and CABINEX 2009. Distinct differences in the magnitudes of important RO_x radical initiation routes (Figs. 11b and 12b) and distinct trends during the morning and afternoon time periods of the OH radical budget (Figs. 11a and 12a) can be seen for the two years. The total RO_x radical budget for both years (Figs. 11b and 12b) reveals that RO_x radical initiation routes are dominated by photolysis pathways (greater than 70% of total initiation) throughout the day, with a smaller contribution of approximately 20–30% from $\text{O}_3 + \text{alkene}$ reactions. Photolysis of ozone, nitrous acid, formaldehyde, aldehydes, and dicarbonyls all contribute significantly to the total RO_x radical budget in both years, with ozone photolysis contributing 19–34% to RO_x

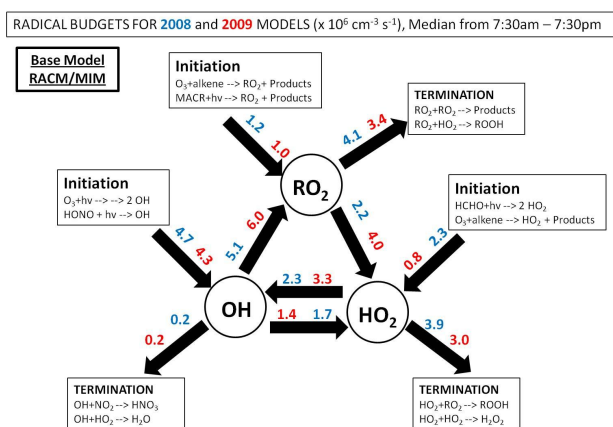


Fig. 10. PROPHET 2008 (blue) and CABINEX 2009 (red) radical budget rates for the time period of 7.30 a.m.–7.30 p.m. Primary reactions contributing to the initiation, termination, and propagation routes are shown in the boxes.

radical initiation and nitrous acid photolysis contributing another 14–20%. The magnitude of the $\text{O}_3 + \text{alkene}$ routes for both years should be interpreted with caution due to the uncertainty associated with the estimations used for many of the unmeasured alkene mixing ratios. The main difference in radical initiation between the PROPHET 2008 and CABINEX 2009 campaigns is the greater contribution of HCHO photolysis to the formation of HO_2 radicals (23% contribution to RO_x radical initiation in 2008 vs. 5% in 2009) due to the higher mixing ratios of HCHO observed in 2008. As mentioned above, the higher HCHO mixing ratios may be a result of the higher mixing ratios of isoprene leading to a greater production of HCHO during the warmer summer of 2008, or the result of greater photochemical activity in 2008 compared to 2009.

RO_x radical termination reactions (Figs. 11b and 12b) are dominated by $\text{RO}_x + \text{RO}_x$ radical reactions throughout the day and night (greater than 90% contribution to total radical termination), due to the relatively low NO_x mixing ratios typically observed at the PROPHET site reducing the importance of the $\text{OH} + \text{NO}_2$ termination reaction. Of the $\text{RO}_x + \text{RO}_x$ termination reactions, $\text{HO}_2 + \text{RO}_2$ reactions dominate at all times due to their larger rate constants (2–3 times greater) compared to the $\text{RO}_2 + \text{RO}_2$ and $\text{HO}_2 + \text{HO}_2$ reactions. In addition, only a fraction of the $\text{RO}_2 + \text{RO}_2$ reaction channels terminate the radicals, although the chemistry for $\text{RO}_2 + \text{RO}_2$ reactions is simplified in RACM.

During CABINEX 2009, rates of RO_x radical propagation were highest in the morning, with the $\text{HO}_2 + \text{NO} \rightarrow \text{OH} + \text{NO}_2$ reaction contributing to approximately 53% of total OH production (Fig. 12a), correlating with the morning NO peak seen in Fig. 3. By afternoon, radical propagation rates generally decreased due to the decrease in NO even though the rate of radical initiation in the afternoon was similar to the morning. Although the median measured mixing

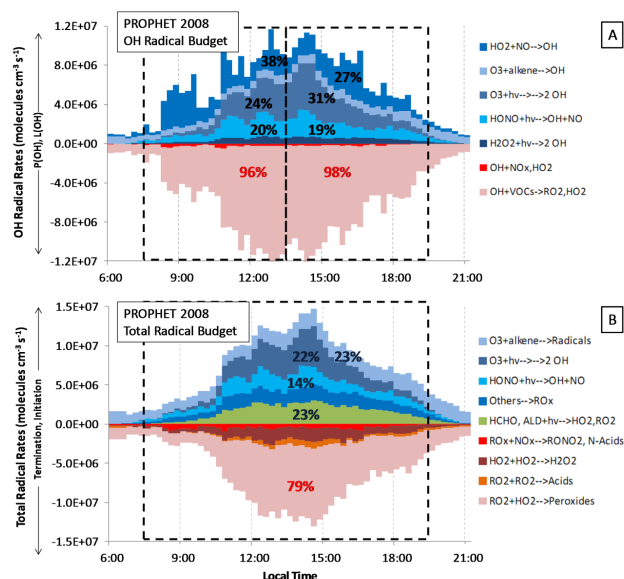


Fig. 11. PROPHET 2008 radical budget diagrams showing the campaign median OH radical budget (A) that compares all the production and loss terms (i.e., initiation, termination, and propagation routes) for OH and the total radical budget (B) that groups and compares all initiation and termination reaction rates for OH, HO_2 , and RO_2 radicals.

ratios of NO were similar during PROPHET 2008 and CABINEX 2009 (Fig. 3), the mixing ratio of NO during periods based on availability and overlap of key constraints results in lower morning mixing ratios of NO constraining the model in 2008 compared to 2009 (Fig. S4). As a result, modeled rates of RO_x radical propagation are lower during the morning in 2008 due to the lower mixing ratios of NO constraining the model (Fig. S4), with the $\text{HO}_2 + \text{NO}$ reaction contributing to approximately 30–40% of the total OH production (Fig. 11a). The propagation of OH to RO_2 radicals is similar in each year except in the morning where this propagation route is 2–6 times higher for CABINEX due to the high NO mixing ratio constraining the model during the days used in this analysis (see Supplement).

The campaign median OH radical budget for CABINEX (Fig. 12a) also illustrates an imbalance between the steady-state HONO production and loss as predicted by the model. The gas-phase HONO source ($\text{OH} + \text{NO} + \text{M} \rightarrow \text{HONO}$) contributes less than 6% from 7.30 a.m.–7.30 p.m. and less than 1% at noontime to the total rate of HONO formation based on the total loss of HONO by photolysis. This imbalance translates to a missing source during CABINEX of approximately 150 pptv h^{-1} on average throughout the day and 250 pptv h^{-1} at noontime. The magnitude of this missing source correlates well ($R^2 = 0.80$) with the measured value of $J(\text{HONO})$ (Fig. S6) suggesting that the missing source is photolytic. These results are consistent with the results of Zhou et al. (2011) who measured an upward flux of HONO

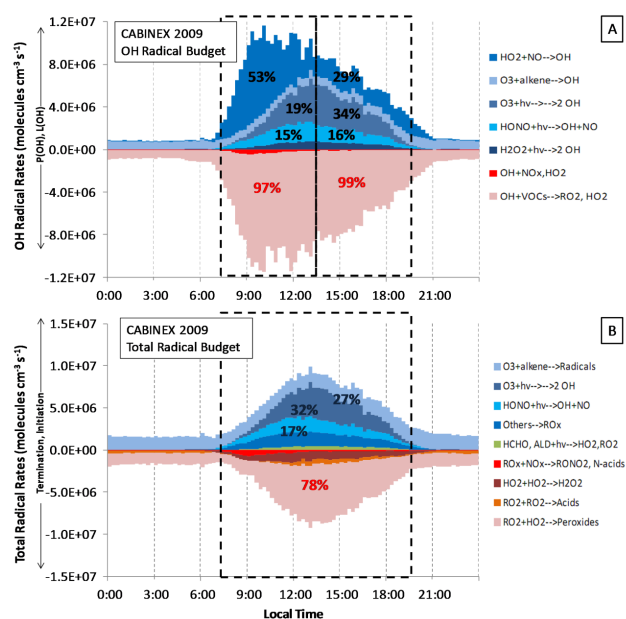


Fig. 12. CABINEX 2009 radical budget diagrams showing the campaign median OH radical budget (A) that compares all the production and loss terms (i.e., initiation, termination, and propagation routes) for OH and the total radical budget (B) that groups and compares all initiation and termination reaction rates for OH, HO₂, and RO₂ radicals.

at the PROPHET site that correlated with leaf-surface nitrate loading and the rate constant of nitrate photolysis. These authors found that this canopy surface source of HONO corresponded to a production rate of approximately 200 pptv h⁻¹ at noontime, contributing to approximately 57 % of the measured total noontime source of HONO in that study (Zhou et al., 2011).

The base-case radical budget from the PROPHET site in 1998 has similarities to both the 2008 and 2009 radical budgets presented here (Tan et al., 2001). The isoprene and HCHO mixing ratios observed in 1998 were similar to the PROPHET 2008 observations, while the NO mixing ratios observed in 1998 were similar to that observed during CABINEX 2009 and PROPHET 2008 (Fig. 3). As a result, the calculated rates of radical propagation during 1998 were similar to that calculated for 2009, while the rate of HO₂ production from HCHO photolysis was similar to that calculated for 2008. Overall the maximum noontime median campaign modeled OH concentration in 1998 was approximately 1–2 × 10⁶ cm⁻³ (Tan et al., 2001), similar to the measured noontime concentrations in 2008 and 2009 (Figs. 5 and 7) although the model used for 1998 contained several additional BVOC reactions. Similarly, the maximum noontime campaign median modeled HO₂ concentration of approximately 4 × 10⁸ cm⁻³ in 1998 is similar to the predicted HO₂ concentrations presented here for 2008 and 2009 (Figs. 5 and 7). Peak isoprene peroxy radical concentrations were predicted

to be approximately 5 × 10⁸ cm⁻³ in 1998 (Tan et al., 2001), resulting in predicted HO₂ + ISOP concentrations similar to that predicted in 2008 and 2009, but higher than HO₂* measurements reported here.

The measured and modeled OH concentrations reported here during 2008 and 2009 are approximately a factor of 2 lower than the values measured at this site in 1998 using the Penn State LIF-FAGE instrument (Tan et al., 2001). However, Mao et al. (2012) recently observed that OH measurements in a ponderosa pine forest using the Penn State LIF-FAGE instrument during the BEARPEX campaign using a chemical modulation technique resulted in measured OH concentrations that were a factor of 2 lower than those obtained using a spectral modulation technique. As a result, it is possible that the measurements made during PROPHET 1998 may have also suffered from a similar interference. As discussed above, it is not clear whether the IU-FAGE instrument suffers from a similar interference even though subsequent chemical modulation tests at this site did not reveal a measurable interference. Additional measurements of HO_x concentrations are still needed to confirm that the measurements are free from unknown interferences. However, as mentioned previously, any interference in the measurements presented here would result in a reduction in the measured OH concentrations, leading to an overprediction by the model. This result would still stand in contrast to the general underprediction of OH measurements in forest environments by current atmospheric chemistry models (Table 1).

5 Summary

Measurements of OH radical concentrations during the PROPHET 2008 and CABINEX 2009 campaigns were generally in good agreement with model predictions using the Regional Atmospheric Chemistry Mechanism updated with the Mainz Isoprene Mechanism. The measurement/model agreement for OH was good (correlation slope = 0.90 ± 0.35) during the CABINEX campaign, when colder temperatures led to lower observed mixing ratios of isoprene, methacrolein, methyl vinyl ketone, and formaldehyde. This result is in contrast to many previous measurements of OH concentrations in forest environments characterized by low NO_x and high isoprene mixing ratios (Tan et al., 2001; Carslaw et al., 2001; Lelieveld et al., 2008; Pugh et al., 2010; Kubistin et al., 2010; Martinez et al., 2010; Whalley et al., 2011) that have generally been greater than predicted using zero dimensional box models and chemical-transport models, including previous measurements at this site (Tan et al., 2001). Similar to the results of Mao et al. (2012) who also found good agreement between their OH measurements and model, the agreement between the measured and modeled OH concentrations suggest that our understanding of the OH radical chemistry of this forested environment may be better than previously believed.

Similar to measurements reported previously (Fuchs et al., 2011) the IU-FAGE instrument used during the PROPHET 2008 and CABINEX 2009 campaigns was sensitive to the detection of alkene-based peroxy radicals in addition to HO₂. As a result, the measured peroxy radical concentrations (HO₂^{*}) reflect the sum of both HO₂ and isoprene-based β-hydroxyalkyl peroxy radicals (HO₂ + ISOP) for this study. During both campaigns, the measured HO₂^{*} concentrations were generally lower than the modeled sum of HO₂ + ISOP, although the agreement is better in 2008 compared to 2009, indicating the possibility of an incomplete characterization of peroxy radical losses in the model. This result is in contrast to previous studies that found measured HO₂ concentrations greater than predicted (Kanaya et al., 2007; Kubistin et al., 2010). However, it is unclear whether the HO₂ measurements in these studies were also subject to interferences from the detection of alkene-based peroxy radicals.

Although the campaign median OH concentrations measured during PROPHET 2008 and CABINEX 2009 are in good agreement with the model in this analysis, the model does underestimate the OH concentrations measured in the afternoon during 2008. This suggests that there could be a missing source of OH radicals during the warmer summer of 2008 when isoprene mixing ratios were higher, and does not rule out the possibility of the existence of radical cycling reactions under low NO_x conditions contributing to the observed OH concentrations under higher isoprene conditions (Lelieveld et al., 2008; Hofzumahaus et al., 2009; Peeters and Muller, 2010). However, it has been recently suggested that OH measurements using laser-induced fluorescence may suffer from an interference related to the oxidation of biogenic VOCs (Mao et al., 2012). The higher temperatures observed in 1998 and 2008 compared to 2009 resulted in higher biogenic VOC emissions which may have impacted the measured OH concentration during those years, and could account for the discrepancy between the observed and modeled OH concentrations. Measurements of OH concentrations on the ground at the PROPHET site in 2010 did not reveal an unknown interference in the IU-FAGE system, resulting in a measured upper limit for unknown interferences of approximately 5×10^5 molecules cm⁻³ based on the uncertainty associated with these tests (see Supplement). However, more measurements in forest environments with higher mixing ratios of biogenic VOCs are still needed to fully describe the potential level of interferences with the LIF-FAGE technique, which may be more prevalent under warmer conditions and higher mixing ratios of biogenic VOCs.

Although the results from this study indicate that the campaign median nighttime OH concentrations measured during CABINEX 2009 were at or below the detection limit of the instrument, additional nighttime measurements are needed to determine if elevated nighttime OH concentrations are possible in this environment or whether they are a result of an instrument artifact. In addition, measurements of HO₂ radicals without the peroxy radical interference are needed to de-

termine whether the model can reproduce the observed HO₂ concentration both during the day and at night, and whether the observed overprediction of the observed HO₂^{*} concentration is due to an overprediction of the concentration of HO₂, isoprene peroxy radicals, or both. The discrepancy between the HO₂^{*} concentrations observed in 2008 and 2009 with the modeled HO₂ + ISOP concentration, and the impact of proposed radical cycling reactions in the isoprene oxidation mechanism will be further examined in a subsequent paper (Griffith et al., 2013).

Supplementary material related to this article is available online at: <http://www.atmos-chem-phys.net/13/5403/2013/acp-13-5403-2013-supplement.pdf>.

Acknowledgements. This research was supported by grants from the National Science Foundation (AGS-0612738 and AGS-0904167 and AGS 0904134). SG and RH acknowledge support from a Biosphere Atmosphere Research and Training (BART) fellowship.

Edited by: A. Hofzumahaus

References

- Alaghmand, M., Shepson, P. B., Starn, T. K., Jobson, B. T., Wallace, H. W., Carroll, M. A., Bertman, S. B., Lamb, B., Edburg, S. L., Zhou, X., Apel, E., Riemer, D., Stevens, P., and Keutsch, F.: The Morning NO_x maximum in the forest atmosphere boundary layer, *Atmos. Chem. Phys. Discuss.*, 11, 29251–29282, doi:10.5194/acpd-11-29251-2011, 2011.
- Blanch, J. S., Llusia, J., Niinemets, U., Noe, S. M., and Penuelas, J.: Instantaneous and historical temperature effects on alpha-pinene emissions in *Pinus halepensis* and *Quercus ilex*, *J. Environ. Biol.*, 32, 1–6, 2011.
- Bryan, A. M., Bertman, S. B., Carroll, M. A., Dusanter, S., Edwards, G. D., Forkel, R., Griffith, S., Guenther, A. B., Hansen, R. F., Helmig, D., Jobson, B. T., Keutsch, F. N., Lefer, B. L., Pressley, S. N., Shepson, P. B., Stevens, P. S., and Steiner, A. L.: In-canopy gas-phase chemistry during CABINEX 2009: sensitivity of a 1-D canopy model to vertical mixing and isoprene chemistry, *Atmos. Chem. Phys.*, 12, 8829–8849, doi:10.5194/acp-12-8829-2012, 2012.
- Butler, T. M., Taraborrelli, D., Brühl, C., Fischer, H., Harder, H., Martinez, M., Williams, J., Lawrence, M. G., and Lelieveld, J.: Improved simulation of isoprene oxidation chemistry with the ECHAM5/MESy chemistry-climate model: lessons from the GABRIEL airborne field campaign, *Atmos. Chem. Phys.*, 8, 4529–4546, doi:10.5194/acp-8-4529-2008, 2008.
- Cantrell, C. A.: Technical Note: Review of methods for linear least-squares fitting of data and application to atmospheric chemistry problems, *Atmos. Chem. Phys.*, 8, 5477–5487, doi:10.5194/acp-8-5477-2008, 2008.

- Carroll, M. A., Bertman, S. B., and Shepson, P. B.: Overview of the Program for Research on Oxidants: PHotochemistry, Emissions, and Transport (PROPHET) summer 1998 measurements intensive, *J. Geophys. Res.*, 106, 24275–24288, 2001.
- Carroll, M. A., Ocko, I. B., McNeal, F., Weremijewicz, J., Hogg, A. J., Opoku, N., Bertman, S. B., Neil, L., Fortner, E., Thornberry, T., Town, M. S., Yip, G., and Yageman, L.: An Assessment of Forest Pollutant Exposure Using Back Trajectories, Anthropogenic Emissions, and Ambient Ozone and Carbon Monoxide Measurements, *EOS Trans. AGU* 89(53), Fall Meet. Suppl., Abstract A41H-0227, 2008.
- Carslaw, N., Jacobs, P. J., and Pilling, M. J.: Modeling OH, HO₂, and RO₂ radicals in the marine boundary layer 2. Mechanism reduction and uncertainty analysis, *J. Geophys. Res.*, 104, 30257–30273, 1999.
- Carslaw, N., Creasey, D. J., Harrison, D., Heard, D. E., Hunter, M. C., Jacobs, P. J., Jenkin, M. E., Lee, J. D., Lewis, A. C., Pilling, M. J., Saunders, S. M., and Seakins, P. W.: OH and HO₂ radical chemistry in a forested region of north-western Greece, *Atmos. Environ.*, 35, 4725–4737, 2001.
- Crawford, J., Davis, D., Olson, J., Chen, G., Liu, S., Gregory, G., Barrick, J., Sachse, G., Sandholm, S., Heikes, B., Singh, H., and Blake, D.: Assessment of upper tropospheric HO_x sources over the tropical Pacific based on NASA GTE/PEM data: Net effect on HO_x and other photochemical parameters, *J. Geophys. Res.*, 104, 16255–16273, 1999.
- Creasey, D. J., Heard, D. E., and Lee, J. D.: Eastern Atlantic Spring Experiment 1997 (EASE97) 1. Measurements of OH and HO₂ concentrations at Mace Head, Ireland, *J. Geophys. Res.*, 107, 4091, doi:10.1029/2001jd000892, 2002.
- Crouse, J. D., Paulot, F., Kjaergaard, H. G., and Wennberg, P. O.: Peroxy radical isomerization in the oxidation of isoprene, *Phys. Chem. Chem. Phys.*, 13, 13607–13613, 2011.
- de Gouw, J. and Warneke, C.: Measurement of volatile organic compounds in the Earth's atmosphere using proton transfer reaction mass spectrometry, *Mass Spectrom. Rev.*, 26, 223–257, 2007.
- Di Carlo, P., Brune, W. H., Martinez, M., Harder, H., Leshner, R., Ren, X. R., Thornberry, T., Carroll, M. A., Young, V., Shepson, P. B., Riemer, D., Apel, E., and Campbell, C.: Missing OH reactivity in a forest: Evidence for unknown reactive biogenic VOCs, *Science*, 304, 722–725, 2004.
- Dusanter, S., Vimal, D., and Stevens, P. S.: Technical note: Measuring tropospheric OH and HO₂ by laser-induced fluorescence at low pressure. A comparison of calibration techniques, *Atmos. Chem. Phys.*, 8, 321–340, doi:10.5194/acp-8-321-2008, 2008.
- Dusanter, S., Vimal, D., Stevens, P. S., Volkamer, R., and Molina, L. T.: Measurements of OH and HO₂ concentrations during the MCMA-2006 field campaign – Part 1: Deployment of the Indiana University laser-induced fluorescence instrument, *Atmos. Chem. Phys.*, 9, 1665–1685, doi:10.5194/acp-9-1665-2009, 2009a.
- Dusanter, S., Vimal, D., Stevens, P. S., Volkamer, R., Molina, L. T., Baker, A., Meinardi, S., Blake, D., Sheehy, P., Merten, A., Zhang, R., Zheng, J., Fortner, E. C., Junkermann, W., Dubey, M., Rahn, T., Eichinger, B., Lewandowski, P., Prueger, J., and Holder, H.: Measurements of OH and HO₂ concentrations during the MCMA-2006 field campaign – Part 2: Model comparison and radical budget, *Atmos. Chem. Phys.*, 9, 6655–6675, doi:10.5194/acp-9-6655-2009, 2009b.
- Emmerson, K. M., Carslaw, N., Carslaw, D. C., Lee, J. D., McFiggans, G., Bloss, W. J., Gravestock, T., Heard, D. E., Hopkins, J., Ingham, T., Pilling, M. J., Smith, S. C., Jacob, M., and Monks, P. S.: Free radical modelling studies during the UK TORCH Campaign in Summer 2003, *Atmos. Chem. Phys.*, 7, 167–181, doi:10.5194/acp-7-167-2007, 2007.
- Evans, M. J., Shallcross, D. E., Law, K. S., Wild, J. O. F., Simmonds, P. G., Spain, T. G., Berrisford, P., Methven, J., Lewis, A. C., McQuaid, J. B., Pilling, M. J., Bandy, B. J., Penkett, S. A., and Pyle, J. A.: Evaluation of a Lagrangian box model using field measurements from EASE (Eastern Atlantic Summer Experiment) 1996, *Atmos. Environ.*, 34, 3843–3863, 2000.
- Faloona, I., Tan, D., Brune, W., Hurst, J., Barket, D., Couch, T. L., Shepson, P., Apel, E., Riemer, D., Thornberry, T., Carroll, M. A., Sillman, S., Keeler, G. J., Sagady, J., Hooper, D., and Paterson, K.: Nighttime observations of anomalously high levels of hydroxyl radicals above a deciduous forest canopy, *J. Geophys. Res.*, 106, 24315–24333, 2001.
- Flynn, J., Lefer, B., Rappengluck, B., Leuchner, M., Perna, R., Dibb, J., Ziemba, L., Anderson, C., Stutz, J., Brune, W., Ren, X. R., Mao, J. Q., Luke, W., Olson, J., Chen, G., and Crawford, J.: Impact of clouds and aerosols on ozone production in Southeast Texas, *Atmos. Environ.*, 44, 4126–4133, 2010.
- Fuchs, H., Brauers, T., Dorn, H.-P., Harder, H., Häsel, R., Hofzumahaus, A., Holland, F., Kanaya, Y., Kajii, Y., Kubistin, D., Lou, S., Martinez, M., Miyamoto, K., Nishida, S., Rudolf, M., Schlosser, E., Wahner, A., Yoshino, A., and Schurath, U.: Technical Note: Formal blind intercomparison of HO₂ measurements in the atmosphere simulation chamber SAPHIR during the HO_xComp campaign, *Atmos. Chem. Phys.*, 10, 12233–12250, doi:10.5194/acp-10-12233-2010, 2010.
- Fuchs, H., Bohn, B., Hofzumahaus, A., Holland, F., Lu, K. D., Nehr, S., Rohrer, F., and Wahner, A.: Detection of HO₂ by laser-induced fluorescence: calibration and interferences from RO₂ radicals, *Atmos. Meas. Tech.*, 4, 1209–1225, doi:10.5194/amt-4-1209-2011, 2011.
- Geiger, H., Barnes, I., Bejan, J., Benter, T., and Spittler, M.: The tropospheric degradation of isoprene: an updated module for the regional atmospheric chemistry mechanism, *Atmos. Environ.*, 37, 1503–1519, 2003.
- George, L. A., Hard, T. M., and O'Brien, R. J.: Measurement of free radicals OH and HO₂ in Los Angeles smog, *J. Geophys. Res.*, 104, 11643–11655, 1999.
- Griffith, S. M., Hansen, R. F., Dusanter, S., Stevens, P. S., Alaghmand, M., Bertman, S. B., Carroll, M. A., Erickson, M., Galloway, M., Grossberg, N., Hottle, J., Hou, J., Jobson, B. T., Kamrath, A., Keutsch, F. N., Lefer, B. L., Mielke, L. H., O'Brien, A., Shepson, P. B., Thurlow, M., Wallace, W., Zhang, N., and Zhou, X. L.: OH and HO₂ Radical Chemistry during PROPHET 2008 and CABINEX 2009 – Part 2: Investigation of HO_x Recycling Mechanisms, in preparation, 2013.
- Hansen, R. F., Griffith, S. M., Dusanter, S., Rickly, P., Stevens, P. S., Erickson, M. H., Wallace, W., Jobson, B. T., Flynn, J. H., Grossberg, N., Lefer, B. L., Carroll, M. A., Bertman, S. B., and Shepson, P. B.: Measurements of Total Hydroxyl Radical Reactivity during CABINEX 2009 – Part 1: Field Measurements, in preparation, 2013.
- Heard, D. E. and Pilling, M. J.: Measurement of OH and HO₂ in the troposphere, *Chem. Rev.*, 103, 5163–5198, 2003.

- Hofzumahaus, A., Rohrer, F., Lu, K. D., Bohn, B., Brauers, T., Chang, C. C., Fuchs, H., Holland, F., Kita, K., Kondo, Y., Li, X., Lou, S. R., Shao, M., Zeng, L. M., Wahner, A., and Zhang, Y. H.: Amplified Trace Gas Removal in the Troposphere, *Science*, 324, 1702–1704, 2009.
- Holland, F., Hofzumahaus, A., Schäfer, J., Kraus, A., and Pätz, H. W.: Measurements of OH and HO₂ radical concentrations and photolysis frequencies during BERLIOZ, *J. Geophys. Res.*, 108, 8246, doi:10.1029/2001JD001393, 2003.
- Hottle, J. R., Huisman, A. J., Digangi, J. P., Kammrath, A., Galloway, M. M., Coens, K. L., and Keutsch, F. N.: A Laser Induced Fluorescence-Based Instrument for In-Situ Measurements of Atmospheric Formaldehyde, *Environ. Sci. Technol.*, 43, 790–795, 2009.
- Huang, G., Zhou, X. L., Deng, G. H., Qiao, H. C., and Civerolo, K.: Measurements of atmospheric nitrous acid and nitric acid, *Atmos. Environ.*, 36, 2225–2235, 2002.
- Huisman, A. J., Hottle, J. R., Coens, K. L., DiGangi, J. P., Galloway, M. M., Kammrath, A., and Keutsch, F. N.: Laser-induced phosphorescence for the in situ detection of glyoxal at part per trillion mixing ratios, *Anal. Chem.*, 80, 5884–5891, 2008.
- Jenkin, M. E., Saunders, S. M., Pilling, M. J.: The Tropospheric Degradation of Volatile Organic Compounds: A Protocol for Mechanism Development, *Atmos. Environ.*, 31, 81–104, 1997.
- Jenkin, M. E., Shallcross, D. E., and Harvey, J. N.: Development and application of a possible mechanism for the generation of cis-pinonic acid from the ozonolysis of alpha- and beta-pinene, *Atmos. Environ.*, 34, 2837–2850, 2000.
- Jobson, B. T. and McCoskey, J. K.: Sample drying to improve HCHO measurements by PTR-MS instruments: laboratory and field measurements, *Atmos. Chem. Phys.*, 10, 1821–1835, doi:10.5194/acp-10-1821-2010, 2010.
- Kanaya, Y., Sadanaga, Y., Nakamura, K., and Akimoto, H.: Development of a ground-based LIF instrument for measuring HO_x radicals: instrumentation and calibration, *J. Atmos. Chem.*, 38, 73–110, 2001.
- Kanaya, Y., Nakamura, K., Kato, S., Matsumoto, J., Tanimoto, H., and Akimoto, H.: Nighttime variations in HO₂ radical mixing ratios at Rishiri Island observed with elevated monoterpene mixing ratios, *Atmos. Environ.*, 36, 4929–4940, 2002.
- Kanaya, Y. G., Cao, R. Q., Kato, S. G., Miyakawa, Y. K., Kajii, Y., Tanimoto, H., Yokouchi, Y., Mochida, M., Kawamura, K., and Akimoto, H.: Chemistry of OH and HO₂ radicals observed at Rishiri Island, Japan, in September 2003: Missing daytime sink of HO₂ and positive nighttime correlations with monoterpenes, *J. Geophys. Res.*, 112, D11308, doi:10.1029/2006jd007987, 2007.
- Karl, M., Dorn, H. P., Holland, F., Koppmann, R., Poppe, D., Rupp, L., Schaub, A., and Wahner, A.: Product study of the reaction of OH radicals with isoprene in the atmosphere simulation chamber SAPHIR, *J. Atmos. Chem.*, 55, 167–187, 2006.
- Konrad, S., Schmitz, T., Buers, H. J., Houben, N., Mannschreck, K., Mihelcic, D., Musgen, P., Patz, H. W., Holland, F., Hofzumahaus, A., Schafer, H. J., Schroder, S., Volz-Thomas, A., Bachmann, K., Schlomski, S., Moortgat, G., and Grossmann, D.: Hydrocarbon measurements at Pabstthum during the BERLIOZ campaign and modeling of free radicals, *J. Geophys. Res.*, 108, 8251, doi:10.1029/2001jd000866, 2003.
- Kubistin, D., Harder, H., Martinez, M., Rudolf, M., Sander, R., Bozem, H., Eerdeken, G., Fischer, H., Gurk, C., Klüpfel, T., Königstedt, R., Parchatka, U., Schiller, C. L., Stickler, A., Taraborrelli, D., Williams, J., and Lelieveld, J.: Hydroxyl radicals in the tropical troposphere over the Suriname rainforest: comparison of measurements with the box model MECCA, *Atmos. Chem. Phys.*, 10, 9705–9728, doi:10.5194/acp-10-9705-2010, 2010.
- Lelieveld, J., Butler, T. M., Crowley, J. N., Dillon, T. J., Fischer, H., Ganzeveld, L., Harder, H., Lawrence, M. G., Martinez, M., Taraborrelli, D., and Williams, J.: Atmospheric oxidation capacity sustained by a tropical forest, *Nature*, 452, 737–740, 2008.
- Lu, K. D., Rohrer, F., Holland, F., Fuchs, H., Bohn, B., Brauers, T., Chang, C. C., Häseler, R., Hu, M., Kita, K., Kondo, Y., Li, X., Lou, S. R., Nehr, S., Shao, M., Zeng, L. M., Wahner, A., Zhang, Y. H., and Hofzumahaus, A.: Observation and modelling of OH and HO₂ concentrations in the Pearl River Delta 2006: a missing OH source in a VOC rich atmosphere, *Atmos. Chem. Phys.*, 12, 1541–1569, doi:10.5194/acp-12-1541-2012, 2012.
- Madronich, S. and Weller, G.: Numerical-integration errors in calculated tropospheric photodissociation rate coefficients, *J. Atmos. Chem.*, 10, 289–300, 1990.
- Mao, J., Ren, X., Zhang, L., Van Duin, D. M., Cohen, R. C., Park, J.-H., Goldstein, A. H., Paulot, F., Beaver, M. R., Crouse, J. D., Wennberg, P. O., DiGangi, J. P., Henry, S. B., Keutsch, F. N., Park, C., Schade, G. W., Wolfe, G. M., Thornton, J. A., and Brune, W. H.: Insights into hydroxyl measurements and atmospheric oxidation in a California forest, *Atmos. Chem. Phys.*, 12, 8009–8020, doi:10.5194/acp-12-8009-2012, 2012.
- Martinez, M., Harder, H., Ren, X., Leshner, R. L., and Brune, W. H.: Measuring atmospheric naphthalene with laser-induced fluorescence, *Atmos. Chem. Phys.*, 4, 563–569, doi:10.5194/acp-4-563-2004, 2004.
- Martinez, M., Harder, H., Kubistin, D., Rudolf, M., Bozem, H., Eerdeken, G., Fischer, H., Klüpfel, T., Gurk, C., Königstedt, R., Parchatka, U., Schiller, C. L., Stickler, A., Williams, J., and Lelieveld, J.: Hydroxyl radicals in the tropical troposphere over the Suriname rainforest: airborne measurements, *Atmos. Chem. Phys.*, 10, 3759–3773, doi:10.5194/acp-10-3759-2010, 2010.
- Mather, J. H., Stevens, P. S., and Brune, W. H.: OH and HO₂ measurements using laser-induced fluorescence, *J. Geophys. Res.*, 102, 6427–6436, 1997.
- Mielke, L. H., Pratt, K. A., Shepson, P. B., McLuckey, S. A., Wisthaler, A., and Hansel, A.: Quantitative Determination of Biogenic Volatile Organic Compounds in the Atmosphere Using Proton-Transfer Reaction Linear Ion Trap Mass Spectrometry, *Anal. Chem.*, 82, 7952–7957, 2010.
- Mihele, C. M. and Hastie, D. R.: Radical chemistry at a forested continental site: Results from the PROPHET 1997 campaign, *J. Geophys. Res.*, 108, 4450, doi:10.1029/2002jd002888, 2003.
- Millet, D. B., Jacob, D. J., Boersma, K. F., Fu, T. M., Kurosu, T. P., Chance, K., Heald, C. L., and Guenther, A.: Spatial distribution of isoprene emissions from North America derived from formaldehyde column measurements by the OMI satellite sensor, *J. Geophys. Res.*, 113, D02307, doi:10.1029/2007jd008950, 2008.
- Monson, R. K., Harley, P. C., Litvak, M. E., Wildermuth, M., Guenther, A. B., Zimmerman, P. R., and Fall, R.: Environmental and developmental controls over the seasonal pattern of isoprene emission from aspen leaves, *Oecologia*, 99, 260–270, 1994.

- Neuroth, R., Dorn, H.-P., and Platt, U.: High resolution spectral features of a series of aromatic hydrocarbons and BrO: Potential interferences in the atmospheric OH-measurements, *J. Atmos. Chem.* 12, 278–298, 1991.
- Olson, J. R., Crawford, J. H., Chen, G., Fried, A., Evans, M. J., Jordan, C. E., Sandholm, S. T., Davis, D. D., Anderson, B. E., Avery, M. A., Barrick, J. D., Blake, D. R., Brune, W. H., Eisele, F. L., Flocke, F., Harder, H., Jacob, D. J., Kondo, Y., Lefer, B. L., Martinez, M., Mauldin, R. L., Sachse, G. W., Shetter, R. E., Singh, H. B., Talbot, R. W., and Tan, D.: Testing fast photochemical theory during TRACE-P based on measurements of OH, HO₂, and CH₂O, *J. Geophys. Res.*, 109, D15S10, doi:10.1029/2003jd004278, 2004.
- Ortega, J., Helmig, D., Guenther, A., Harley, P., Pressley, S., and Vogel, C.: Flux estimates and OH reaction potential of reactive biogenic volatile organic compounds (BVOCs) from a mixed northern hardwood forest, *Atmos. Environ.*, 41, 5479–5495, 2007.
- Paulot, F., Crouse, J. D., Kjaergaard, H. G., Kurten, A., St.Clair, J. M., Seinfeld, J. H., and Wennberg, P. O.: Unexpected Epoxide Formation in the Gas-Phase Photooxidation of Isoprene, *Science*, 325, 730–733, 2009.
- Peeters, J. and Muller, J. F.: HO_x radical regeneration in isoprene oxidation via peroxy radical isomerisations. II: experimental evidence and global impact, *Phys. Chem. Chem. Phys.*, 12, 14227–14235, 2010.
- Peeters, J., Nguyen, T. L., and Vereecken, L.: HO_x radical regeneration in the oxidation of isoprene, *Phys. Chem. Chem. Phys.*, 11, 5935–5939, 2009.
- Petron, G., Harley, P., Greenberg, J., and Guenther, A.: Seasonal temperature variations influence isoprene emission, *Geophys. Res. Lett.*, 28, 1707–1710, 2001.
- Pöschl, U., von Kuhlmann, R., Poisson, N., and Crutzen, P. J.: Development and intercomparison of condensed isoprene oxidation mechanisms for global atmospheric modeling, *J. Atmos. Chem.*, 37, 29–52, 2000.
- Pugh, T. A. M., MacKenzie, A. R., Hewitt, C. N., Langford, B., Edwards, P. M., Furneaux, K. L., Heard, D. E., Hopkins, J. R., Jones, C. E., Karunaharan, A., Lee, J., Mills, G., Misztal, P., Moller, S., Monks, P. S., and Whalley, L. K.: Simulating atmospheric composition over a South-East Asian tropical rainforest: performance of a chemistry box model, *Atmos. Chem. Phys.*, 10, 279–298, doi:10.5194/acp-10-279-2010, 2010.
- Qi, B., Kanaya, Y., Takami, A., Hatakeyama, S., Kato, S., Sadanaga, Y., Tanimoto, H., and Kajii, Y.: Diurnal peroxy radical chemistry at a remote coastal site over the sea of Japan, *J. Geophys. Res.*, 112, D17306, doi:10.1029/2006jd008236, 2007.
- Ren, X. R., Harder, H., Martinez, M., Faloona, I. C., Tan, D., Leshner, R. L., Di Carlo, P., Simpas, J. B., and Brune, W. H.: Interference Testing for Atmospheric HO_x Measurements by Laser-induced Fluorescence, *J. Atmos. Chem.*, 47, 169–190, 2004.
- Ren, X. R., Brune, W. H., Oliger, A., Metcalf, A. R., Simpas, J. B., Shirley, T., Schwab, J. J., Bai, C. H., Roychowdhury, U., Li, Y. Q., Cai, C. X., Demerjian, K. L., He, Y., Zhou, X. L., Gao, H. L., and Hou, J.: OH, HO₂, and OH reactivity during the PMTACS-NY Whiteface Mountain 2002 campaign: Observations and model comparison, *J. Geophys. Res.*, 111, D10S03, doi:10.1029/2005jd006126, 2006.
- Ren, X. R., Olson, J. R., Crawford, J. H., Brune, W. H., Mao, J. Q., Long, R. B., Chen, Z., Chen, G., Avery, M. A., Sachse, G. W., Barrick, J. D., Diskin, G. S., Huey, L. G., Fried, A., Cohen, R. C., Heikes, B., Wennberg, P. O., Singh, H. B., Blake, D. R., and Shetter, R. E.: HO_x chemistry during INTEX-A 2004: Observation, model calculation, and comparison with previous studies, *J. Geophys. Res.*, 113, D05310, doi:10.1029/2007jd009166, 2008.
- Ren, X., Mao, J., Brune, W. H., Cantrell, C. A., Mauldin III, R. L., Hornbrook, R. S., Kosciuch, E., Olson, J. R., Crawford, J. H., Chen, G., and Singh, H. B.: Airborne intercomparison of HO_x measurements using laser-induced fluorescence and chemical ionization mass spectrometry during ARCTAS, *Atmos. Meas. Tech.*, 5, 2025–2037, doi:10.5194/amt-5-2025-2012, 2012.
- Sander, S. P., Friedl, R. R., Golden, D. M., Kurylo, M. J., Huie, R. E., Orkin, V. L., Moortgat, G. K., Ravishankara, A. R., Kolb, C. E., Molina, M. J., and Finlayson-Pitts, B. J.: Chemical Kinetics and Photochemical Data for Use in Atmospheric Studies, Evaluation Number 14, JPL Publication 02-25, NASA Jet Propulsion Laboratory, Pasadena, California, 2003.
- Sander, S. P., Friedl, R. R., Barker, J. R., Golden, D. M., Kurylo, M. J., Wine, P. H., Abbatt, J. P. D., Burkholder, J. B., Kolb, C. E., Moortgat, G. K., Huie, R. E., and Orkin, V. L.: Chemical Kinetics and Photochemical Data for Use in Atmospheric Studies, Evaluation Number 17, JPL Publication 10-6, NASA Jet Propulsion Laboratory, Pasadena, California, 2011.
- Saunders, S. M., Jenkin, M. E., Derwent, R. G., and Pilling, M. J.: Protocol for the development of the Master Chemical Mechanism, MCM v3 (Part A): tropospheric degradation of non-aromatic volatile organic compounds, *Atmos. Chem. Phys.*, 3, 161–180, doi:10.5194/acp-3-161-2003, 2003.
- Schlosser, E., Brauers, T., Dorn, H.-P., Fuchs, H., Häsel, R., Hofzumahaus, A., Holland, F., Wahner, A., Kanaya, Y., Kajii, Y., Miyamoto, K., Nishida, S., Watanabe, K., Yoshino, A., Kubistin, D., Martinez, M., Rudolf, M., Harder, H., Berresheim, H., Elste, T., Plass-Dülmer, C., Stange, G., and Schurath, U.: Technical Note: Formal blind intercomparison of OH measurements: results from the international campaign HO_xComp, *Atmos. Chem. Phys.*, 9, 7923–7948, doi:10.5194/acp-9-7923-2009, 2009.
- Sharkey, T. D. and Yeh, S. S.: Isoprene emission from plants, *Annu. Rev. Plant Physiol. Plant Mol. Biol.*, 52, 407–436, 2001.
- Stavrakou, T., Peeters, J., and Müller, J.-F.: Improved global modelling of HO_x recycling in isoprene oxidation: evaluation against the GABRIEL and INTEX-A aircraft campaign measurements, *Atmos. Chem. Phys.*, 10, 9863–9878, doi:10.5194/acp-10-9863-2010, 2010.
- Stevens, P. S., Mather, J. H., and Brune, W. H.: Measurement of tropospheric OH and HO₂ by laser-induced fluorescence at low pressure, *J. Geophys. Res.*, 99, 3543–3557, 1994.
- Stockwell, W. R., Kirchner, F., Kuhn, M., and Seefeld, S.: A new mechanism for regional atmospheric chemistry modeling, *J. Geophys. Res.*, 102, 25847–25879, 1997.
- Stockwell, W. R., Goliff, W. S., Pinder, R. W., Sarwar, G., Mathur, R., Schere, K. L., and Fahr, A.: A model comparison of nitrogen-containing compounds in the free troposphere using three mechanisms: RACM2, CB05 and SAPRC99, *EOS Trans. AGU* 89(53), Fall Meet. Suppl., Abstract A54C-08, 2008.
- Tan, D., Faloona, I., Simpas, J. B., Brune, W., Shepson, P. B., Couch, T. L., Sumner, A. L., Carroll, M. A., Thornberry, T., Apel, E., Riemer, D., and Stockwell, W.: HO_x budgets in a deciduous forest: Results from the PROPHET summer 1998 campaign, *J. Geophys. Res.*, 106, 24407–24427, 2001.

- Taraborrelli, D., Lawrence, M. G., Butler, T. M., Sander, R., and Lelieveld, J.: Mainz Isoprene Mechanism 2 (MIM2): an isoprene oxidation mechanism for regional and global atmospheric modelling, *Atmos. Chem. Phys.*, 9, 2751–2777, doi:10.5194/acp-9-2751-2009, 2009.
- Whalley, L. K., Edwards, P. M., Furneaux, K. L., Goddard, A., Ingham, T., Evans, M. J., Stone, D., Hopkins, J. R., Jones, C. E., Karunaharan, A., Lee, J. D., Lewis, A. C., Monks, P. S., Moller, S. J., and Heard, D. E.: Quantifying the magnitude of a missing hydroxyl radical source in a tropical rainforest, *Atmos. Chem. Phys.*, 11, 7223–7233, doi:10.5194/acp-11-7223-2011, 2011.
- Wild, O., Law, K. S., McKenna, D. S., Bandy, B. J., Penkett, S. A., and Pyle, J. A.: Photochemical trajectory modeling studies of the North Atlantic region during August 1993, *J. Geophys. Res.*, 101, 29269–29288, 1996.
- Zhou, X. L., Zhang, N., TerAvest, M., Tang, D., Hou, J., Bertman, S., Alaghmand, M., Shepson, P. B., Carroll, M. A., Griffith, S., Dusanter, S., and Stevens, P. S.: Nitric acid photolysis on forest canopy surface as a source for tropospheric nitrous acid, *Nature Geosci.*, 4, 440–443, 2011.